GENETICS, 2026, 233(1), iyag049
https://doi.org/10.1093/genetics/iyag049
Advance Access Publication Date: 26 February 2026
Investigation

Retinoic acid production via the ray-finned fish gene *bco1l* is essential for juvenile development

Lochlan Sife Krupa,[1,2,3] Paula R. Villamayor,[1,2,3] Sepalika Bandara,[4] Yanqi Zhang,[4] Alec Palmiotti,[1,2,3] Johannes von Lintig ,[4] Andres Bendesky [1,2,3,*]

[1]Zuckerman Mind Brain Behavior Institute, Columbia University, 3227 Broadway, New York, NY 10027, United States
[2]Department of Ecology, Evolution and Environmental Biology, Columbia University, Schermerhorn Extension 10th Floor, 1200 Amsterdam Ave, New York, NY 10027, United States
[3]Kavli Institute for Brain Science, Columbia University, 3227 Broadway, New York, NY 10027, United States
[4]Department of Pharmacology, Case Western Reserve University, 10900 Euclid Ave, Cleveland, OH 44106, United States

*Corresponding author: Zuckerman Mind Brain Behavior Institute, Columbia University, 3227 Broadway, New York, NY 10027, United States. Email: a.bendesky@columbia.edu; Bluesky: @bendeskylab.com

In vertebrates, vitamin A (VA) is crucial for development, tissue homeostasis, vision, and immunity. Retinal, a form of VA, can be produced via enzymatic cleavage of β-carotene by *beta-carotene oxygenase 1* (*bco1*) and *bco1-like* (*bco1l*), but the developmental and tissue-specific functions of these genes are poorly understood. While *bco1* is found across vertebrate taxa, *bco1l* is a paralog of *bco1* that we discover to have evolved in the ray-finned fishes, the most abundant, speciose, and commercially important group of fishes. We investigated the function of *bco1l* in ray-finned Siamese fighting fish, commonly known as betta, an emerging model for genetics and development. Using CRISPR/Cas9 knockouts, we find that lack of *bco1l* results in reduced VA and elevated β-carotene in larvae, starting when animals have exhausted their yolk supply of retinal, followed by stunted growth and death during juvenile development. Exogenous retinoic acid largely rescues the mutation, demonstrating its deficiency causes these defects. *bco1l* is 7× more abundant than *bco1* in the intestine. This, coupled with the inability of *bco1* to sustain VA production in the *bco1l* mutant, indicates that *bco1l* is the primary enzyme for dietary carotenoid conversion into retinal. Our results show that VA production by *bco1l* is required for post-embryonic development, and that *bco1l* became essential after evolving via duplication of *bco1*.

Keywords: vitamin A; retinoic acid; betta fish; development; paralog; evolution

Introduction

Vitamin A (VA) deficiency has detrimental consequences, including improper pattern formation during development, stunted growth, compromised immunity, and impaired vision including blindness (Clagett-Dame and DeLuca 2002; Huang et al. 2018; Hernandez and Hardy 2020; Menezes and Almeida 2024). To prevent such defects, VA must be obtained preformed from the diet or enzymatically produced through the conversion of dietary pro-VA carotenoids (O'Byrne and Blaner 2013).

Due to their biological activities, carotenoids have a variety of applications. They are commonly employed as food supplements in aquaculture, where they are used to enhance animal coloration and growth (Liao et al. 2025). Carotenoids also have applications in medicine, including boosting immune function, reducing the risk of chronic disease, and treating VA deficiency (von Lintig 2010; Vílchez et al. 2011; Metibemu and Ogungbe 2022).

In vertebrates, the enzyme beta-carotene oxygenase 1 (encoded by the *bco1* gene) catalyzes the cleavage of the carotenoid β-carotene into two molecules of retinal (retinaldehyde), a form of VA, via 15,15′ oxygenase activity (Fig. 1; Wyss et al. 2000; Harrison and Kopec 2020). Retinal is then irreversibly oxidized to the biologically active metabolite retinoic acid (RA) or reduced to retinol. Retinol can be further converted into retinyl esters, which are storage forms of VA (von Lintig 2010; O'Byrne and Blaner 2013). Retinyl esters also serve as precursors of the visual chromophore (11-*cis* retinal) (Kiser et al. 2014). *bco1* is expressed in the epithelium of the small intestinal mucosa, where it contributes to producing VA from dietary β-carotene (Goodman and Huang 1965; Olson and Hayaishi 1965; Lindqvist and Andersson 2002; Takitani et al. 2006). This intestinal-derived VA is typically stored in the liver as retinyl esters (Lindqvist and Andersson 2004; von Lintig et al. 2005). *bco1* is also expressed in other tissues including the kidneys, lungs, liver, and retina, where it likely provides VA locally (Paik et al. 2001; Wyss et al. 2001; Yan et al. 2001; Lindqvist and Andersson 2004; Mora et al. 2004). Knockout of *bco1* in mice results in the accumulation of β-carotene, a reduction of VA stores, and an exacerbation of defects resulting from VA deficiency during embryonic development (Hessel et al. 2007; Kim et al. 2011). Morpholino-mediated knockdown of *bco1* in zebrafish (*Danio rerio*) results in malformation of neural crest derivatives such as the mandible and pigment cells during embryonic development (Lampert et al. 2003). However, a CRISPR/Cas9-mediated loss-of-function mutation in *bco1* in the closely related pearl danio (*Danio albolineatus*) only leads to a subtle pigmentation phenotype in adults (Huang et al. 2021). Therefore, the function of *bco1* in fish might be particularly important in tissues derived from the neural crest.

Received on 03 October 2025; accepted on 13 February 2026
Published by Oxford University Press on behalf of The Genetics Society of America 2026.
This work is written by (a) US Government employee(s) and is in the public domain in the US.

Downloaded from academic.oup.com/genetics/article/233/1/iyag049/8498880 by Columbia University Libraries user on 04 October 2026

Beta-carotene oxygenase 1-like (*bco1l*) is a paralog of *bco1* found in ray-finned fishes (Actinopterygii) (Helgeland et al. 2014). Like *bco1*, *bco1l* also catalyzes the symmetric cleavage of β-carotene to retinal (Fig. 1; Helgeland et al. 2019; Kwon et al. 2022). The presence of *bco1l* across ray-finned fishes is notable given that one of a pair of paralogous genes is typically pseudogenized following duplication (Lynch and Conery 2000). The preservation of both *bco1* and *bco1l* suggests that subfunctionalization (the division of the functions of the ancestral and derived paralogs) or neofunctionalization (the emergence of a novel function for one of the paralogs) may have occurred (Magadum et al. 2013). Several studies in Atlantic salmon provide preliminary evidence for the subfunctionalization of *bco1* and *bco1l*. The two genes display differential expression in the intestine, liver, and muscle (Helgeland et al. 2014) and may have distinct impacts on carotenoid deposition in muscle (Helgeland et al. 2019; Kuhn 2022). However, duplicate genes can be maintained for extended periods of time through processes such as dosage-balance selection and hypofunctionalization without undergoing subfunctionalization (Qian et al. 2010; Wilson and Liberles 2023), and the relative expression of paralogous genes can be subject to drift (Thompson et al. 2016). To date, functional roles and evolutionary trajectories of *bco1* and *bco1l* in ray-finned fishes remain largely unknown.

We previously used CRISPR/Cas9 to knock out *bco1l* in betta fish and observed that the homozygous mutant genotype was lethal (Palmiotti et al. 2023). In this study, we sought to characterize the developmental and biochemical phenotypes of the knockout and to parse the evolution and respective roles of *bco1* and *bco1l* in carotenoid metabolism and VA production.

Materials and methods

Animal husbandry

Fish care followed our previously published protocols (Lichak et al. 2022), unless otherwise specified. Columbia University Institutional Animal Care and Use Committee approved all animal protocols. We began feeding larvae with *Brachionus rotundiformis* rotifers at 5 dpf. Rotifers were raised in reverse-osmosis (RO) water raised to a salinity of 15 ppt with Instant Ocean aquarium salt. We fed rotifers algae (Lichak et al. 2022). Each day, we decanted 4 L of a 200 to 600 rotifer/mL solution through a 41 µm sieve and resuspended rotifers in 250 mL of rotifer water in a 1 L beaker. We then mixed 25 mL aliquots of this concentrated solution with 175 mL of fish water (Lichak et al. 2022). We fed this solution to our larval fish once per day (~6.7 mL per fish). We transitioned betta to newly hatched brine shrimp (*Artemia nauplii*) at 15 dpf. We used E-Z Egg brine shrimp eggs (Brine Shrimp Direct, Ogden, UT, USA). We seeded egg batches daily by adding 45 mL of E-Z Eggs to 16 L of RO water with 2 cups of Instant Ocean aquarium salt in a 16 L acrylic hatching cone. We allowed 18 to 24 h for hatching prior to harvest, then drained the water through a 120 µm screen. We then resuspended hatched brine shrimp in 1 L of RO water. We stored brine shrimp at 4 °C for up to 24 h (until the next harvest). Apart from experiments in which we individually housed larvae (see "Survey through development" and "Retinoic acid treatment"), we fed fish with *Artemia* twice per day (~0.35 mL of the resuspended hatched brine shrimp per fish per feeding) from 15 to 29 dpf. From 30 to 79 dpf, we fed fish *Artemia* 3 times per day (~0.35 to 1 mL per fish per feeding) and Golden Pearl Reef and Larval Fish pellets (Brine Shrimp Direct, Ogden, UT) once per day (100 to 300 µm; 3 to 9 mg per fish). From 80 dpf onwards, we fed individually housed adult fish ~10 mL of *Artemia* and 3 to 5 Golden Pearl fish pellets (300 to 800 µm diameter) once per day.

Genotyping

To extract DNA, we digested fin clips or whole larvae samples in 20 µL of a Proteinase K working buffer (10 mM Tris (pH 8), 2 mM EDTA, 0.2% Triton-X, 2 µg Proteinase K (D3001-2-H, Zymo Research)) at 65 °C for 40 min followed by 95 °C for 10 min. We used the lysate directly for genotyping. In cases where we also extracted RNA, we obtained DNA and RNA from tissue samples using the Quick-DNA/RNA Microprep Plus Kit (D7005, Zymo Research). Prior to all fin clip procedures, we anesthetized fish in a 0.8% tricaine methanesulfonate (MS-222) solution in fish water.

For wild-type +/+ × heterozygous +/− outcrosses, we used a T7 endonuclease assay (Mashal et al. 1995; Sentmanat et al. 2018) (M0302, New England Biolabs). We amplified *bco1l* from genomic DNA using the following primers: CAGATCCCTGCCAGAACATT and TGAGCCTGTGGTTCACTGAC. We induced hybridization by running 10 µL unpurified PCR product with 7.75 µl water and 2 µl NEB Buffer 2 (B6002, New England Biolabs) in the following conditions: 98 °C (5 min), 95 to 85 °C (−2 °C/sec), 85 to 25 °C (−0.1 °C/sec). We then added 0.25 µl T7 Endonuclease I directly to each of the hybridized samples and incubated at 37 °C for 60 min. T7 endonuclease I cuts heteroduplex DNA (arising from heterozygosity), which we visualized after electrophoresis in a 1.5% agarose gel.

For +/− × +/− crosses, we genotyped offspring using a digital PCR assay with primers specific to *bco1l* (CCGCTATGGTG ACGACTACTAC and TGCCGACAGTTTCCAAGGT) and probes specific to the wild and mutant alleles (Wild: /56-FAM/TCCTCT GAGATCAAC/3MGB-NFQ/; Mutant: /5SUN/CTCCTCTGATGATC AAC/3MGB-NFQ/). We performed all reactions using a QIAcuity digital PCR system (QIAGEN) and 8.5 k partition dPCR plates. We used either a TaqMan probe mix (Thermo Fisher Scientific) or reconstituted probes and primers from Integrated DNA Technologies (IDT). For the TaqMan probes, we used a 14 µL reaction volume with the following reagent concentrations: 3.75 µL 40× QIAcuity Probe Mastermix (250102, QIAGEN), 0.375 µL 40× TaqMan assay mix, 8.875 µL RNase/DNase-free water, and 1 µL template DNA (6 ng/µL for extracted DNA or 1 µL of product solution from the Proteinase K digestion). For the IDT probes and primers, we used a 14 µL reaction volume with the following reagent concentrations: 3.75 µL 40× QIAcuity Probe MM, 0.135 µL *bco1l* forward primer (100 µM), 0.135 µL *bco1l* reverse primer (100 µM), 0.03 µL *bco1l* wild-type probe (100 µM), 0.03 µL *bco1l* mutant probe (100 µM), 8.92 µL RNase/DNase-free water, and 1 µL template DNA. We used the QIAGEN Probe Priming protocol and the following cycling conditions: 95 °C (2 min), 40 × [95 °C (15 s), 60 °C (30 s)]. We performed fluorescence imaging with the green (FAM; wild) and yellow (VIC; mutant) channels with an exposure duration of 500 ms and a gain of 6. We set fluorescence thresholds based on the 1D and 2D scatterplots of the data. We included +/+, +/−, and −/− control samples in every run.

Survey through development

We sampled individuals from a +/− × +/− cross at 3, 6, 10, 12, and 20 dpf using a glass Pasteur pipette cut at the taper and flame-smoothed. We imaged each fish using a Leica S9i Stereo Microscope and then genotyped each individual. All images included a ruler to compare length and were scrutinized for evidence of abnormal phenotypes.

At 22 to 24 dpf, we individually housed larvae of all 3 genotypes in 200 to 300 mL of fish water in opaque plastic cups to prevent death due to competition for food. We fed the fish *Artemia* 4× per day (~20 to 50 shrimp per feeding) and replaced the media

Downloaded from academic.oup.com/genetics/article/233/1/iyag049/8498880 by Columbia University Libraries user on 04 October 2026

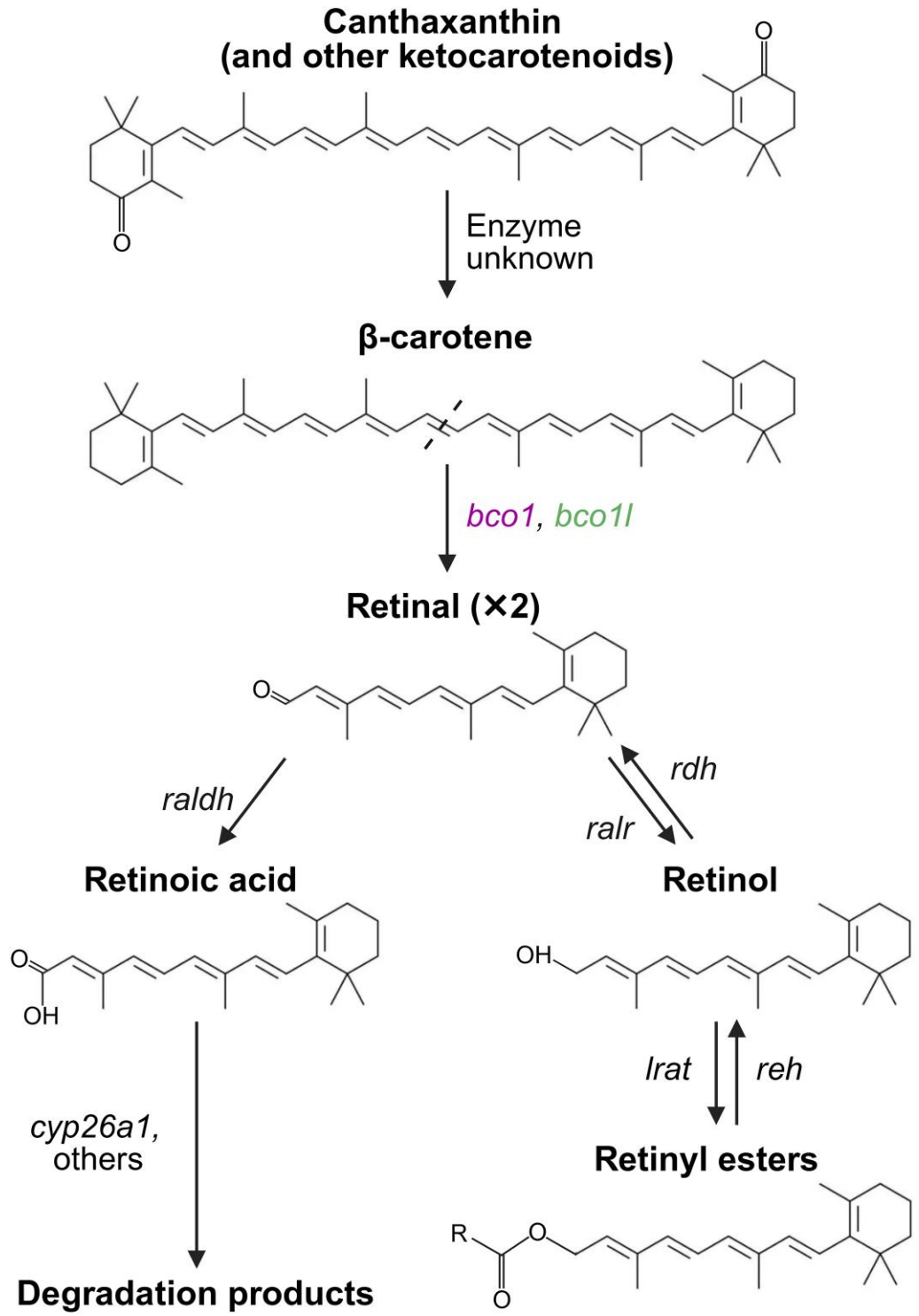

Fig. 1. Metabolism of carotenoids to retinoids in vertebrates. Ketocarotenoids, such as canthaxanthin (pictured), can be converted to β-carotene in some species, though the enzymes involved in this process remain undescribed (Schiedt et al. 1985; Kaisuyama and Matsuno 1988; Yamashita et al. 1996; Sangeetha and Baskaran 2010). β-carotene is converted to two molecules of retinal via the 15,15′oxygenase activity of *bco1*. *bco1l* is also capable of catalyzing this reaction in the ray-finned fishes (Helgeland et al. 2019; Kwon et al. 2022). Retinal is converted to retinoic acid by one of three retinal dehydrogenases (*raldh*) (|Lampert et al. 2003; O'Byrne and Blaner 2013). Retinoic acid is converted to inactive metabolites through the action of cytochrome P450 enzymes including *cyp26a1* (White et al. 1996; Isken et al. 2007). Retinal may also be reversibly reduced to retinol by retinal reductase (*ralr*), which is further acylated to the storage form (retinyl esters) by lecithin:retinol acyltransferase (*lrat*). Retinyl esters are converted to retinol by retinyl ester hydrolase (*reh*), and subsequently oxidized to retinal by one of the retinol dehydrogenase (*rdh*) family members (O'Byrne and Blaner 2013).

every other day. Twice per day, we screened for dead fish. If a fish was found dead, we stored it at −20 °C for genotyping and recorded its age at death. We photographed each fish in the cups top-down at 24, 29, 34, 39, and 44 dpf. We processed the images using ImageJ (Schneider et al. 2012), obtaining length measurements by multiplying the ratio of the number of pixels along the

Downloaded from academic.oup.com/genetics/article/233/1/iyag049/8498880 by Columbia University Libraries user on 04 October 2026

body of the fish to those along the diameter of the bottom of the cup by the known diameter of the cup bottom (4.5 cm). At 90 dpf, we weighed and genotyped all remaining fish. Fish were euthanized via submersion in ice-cold water, patted dry using a Kimwipe, and weighed using a Mettler-Toledo ML104T/00 Analytical Balance. We took all photos and videos using a Canon EOS RP camera with a Canon Macro lens EF 100 mm inside a photo tent illuminated with white light-emitting diodes.

Retinoic acid treatment

We dissolved all-*trans*-Retinoic acid (RA; R2625, Sigma-Aldrich) in dimethyl sulfoxide (DMSO) at a concentration of 0.1 M and stored it in 5 µL aliquots in the dark at −70 °C. Beginning at 5 dpf, we housed treatment larvae in fish water containing 5 nM RA and 0.1% DMSO. Control larvae were housed in 0.1% DMSO. At 10 dpf, we sampled treated individuals and quantified *cyp26a1* expression across the 3 genotypes. To prevent competition for food, we individually housed both the treatment and control fish in plastic cups at 15 dpf containing 200 to 300 mL of fish water. We fed fish with *Artemia* 2× per day (~20 to 50 fish per feeding) and replaced the media every other day. We tracked survival, imaged each fish at 24, 34, and 44 dpf, and obtained length measurements using the same protocol as for the untreated fish (see "Survey through development"). We terminated the experiment at 60 dpf and genotyped and weighed the remaining fish.

Digital PCR for *cyp26a1*, *bco1*, and *bco1l*

We extracted total RNA from whole-body samples of larval fish at 3, 10, and 20 dpf using the Quick-DNA/RNA Microprep Plus Kit (D7005, Zymo Research). We extracted total RNA from eye, gonad, head kidney, intestine, liver, skin, and muscle samples of 5 adult (3 male, 2 female), wild-type betta of the red veil variety using the Quick-RNA Miniprep Kit (R1054, Zymo Research). We quantified RNA using a Nanodrop One (13-400-519, Thermo Fisher Scientific, Waltham, MA) and a Qubit RNA IQ Assay (Q33216, Invitrogen Qubit 3.0 Fluorometer). We synthesized cDNA using the LunaScript RT SuperMix kit (E3010, New England Biolabs).

In larval samples, we quantified *cyp26a1* expression using a PrimeTime qPCR Probe Assay (IDT) with primers (GCTGG TGGAGGCTTTTGAGG, GTGTCGGACTCCTGCACCTT) and probe (/56-FAM/TGTACAGGG/ZEN/GTCTGAAGGCGAGGAA/3IABkFQ/) specific to the mRNA transcript of *cyp26a1*. We quantified *bco1* and *bco1l* expression in adult tissue samples using 2 PrimeTime qPCR Probe Assays (IDT) with primers (*bco1*: TGACACAGA AACCAAGGAACT, GACCGCGCCATCATCTT; *bco1l*: GAGAACTGCT ACCCATCAGAAC, GGAAATGTGAGGATCTGGAGAAA) and probes (*bco1*: /5TexRd-XN/AGACAACTGCTTTCCATCGGAACCA/3BHQ_2/; *bco1l*: /56-FAM/TCACACCAT/ZEN/CATCCTCATCCACAGC/3IABk FQ/) specific to mRNA transcripts of *bco1* and *bco1l*.

We performed all reactions using a QIAcuity digital PCR system and 8.5 k partition dPCR plates. For *cyp26a1*, each reaction contained 50 ng of RNA reverse transcribed into cDNA in a 15 µL solution (0.75 µL 20× qPCR probe mix, 3.75 µL QIAcuity Probe Mastermix, 5 µL 10 ng/µL cDNA template, 5.5 µL RNase/DNase-free water). For tissue-specific *bco1* and *bco1l* expression in adults, we ran multiplexed dPCRs with 40.2 ng RNA/cDNA input in 15 µL of solution (0.75 µL 20× *bco1* qPCR probe mix, 0.75 µL 20× *bco1l* qPCR probe mix, 3.75 µL QIAcuity Probe Mastermix, 6.7 µL 6 ng/µL cDNA template, 3.05 µL RNase/DNase-free water). For *bco1* expression in larvae, we ran multiplexed dPCRs with 50 ng RNA/cDNA input in 15 µL of solution (0.75 µL 20× *bco1* qPCR probe mix, 0.75 µL 20× *bco1l* qPCR probe mix, 3.75 µL QIAcuity Probe Mastermix, 5 µL 10 ng/µL cDNA template, 4.75 µL RNase/DNase-free water). For all dPCR assays, we used the QIAGEN Probe Priming protocol and the following cycling conditions: 95 °C (2 min), 40 × [95 °C (15 s), 60 °C (30 s)]. We performed fluorescence imaging using the green (FAM; *cyp26a1*, *bco1l*) and red (TexRd; *bco1*) channels with an exposure duration of 500 ms and a gain of 6. We set fluorescence thresholds based on the 1D and 2D scatterplots of the data.

HPLC for carotenoid and retinoid concentrations

We collected between 50 and 100 eggs in indirect light within 5 h of mating from each of 4 wild-type betta crosses of the red veil variety. We raised the remaining offspring in low light until 5 dpf and then sampled between 50 and 100 larvae from the same crosses. All samples were counted, pooled, and immediately stored at −70 °C in the dark. We sampled larvae of the *bco1l* knockouts at 20 dpf and genotyped them via a small caudal fin biopsy. We then made pools of 3 to 5 fish of the same genotype. We euthanized larvae via submersion in ice-cold water and patted dry with Kimwipes prior to weighing. We weighed samples using a Mettler-Toledo ML104T/00 Analytical Balance. All pooled samples were between 14 and 26 mg and stored at −70 °C in the dark. We sampled newly hatched brine shrimp and rotifers from our lab cultures, concentrating them into a pellet in a microcentrifuge tube via centrifugation at 20,817 rcf. We removed excess water via a pipette after centrifugation. Samples were between 12 and 25 mg. We note that, while we filtered our rotifer culture through a 41 µm sieve to remove algae, residual algae in our rotifer samples may contribute to the carotenoid content.

We homogenized whole larvae, eggs, brine shrimp, and rotifers using a handheld homogenizer in 100 µL of phosphate-buffered saline (PBS, pH 7.4). We extracted carotenoids and retinoids after the addition of 200 µL 2 M hydroxylamine (pH 6.8) and 200 µL methanol to form the corresponding retinaldehyde oximes (syn and anti). Then, we added 400 µL acetone, followed by sequential extraction by 2 rounds of 500 µL hexane. We separated the organic phase by centrifugation and collected and vacuum-dried it using an Eppendorf vacuum centrifuge.

We reconstituted the debris in a 99:1 (v/v) mixture of hexane and ethyl acetate and subjected it to gradient elution via high-performance liquid chromatography (HPLC). We performed gradient separation in 2 steps: The first utilized a 99:1 (v/v) hexane: ethyl acetate mixture for 10 min, allowing the elution of β-carotene and retinyl esters. The second step employed an 80:20 (v/v) hexane:ethyl acetate mixture for 15 min, facilitating the elution of more polar compounds, including ketocarotenoids, retinal-oximes, and retinol. We conducted HPLC analysis using an Agilent 1260 Infinity Quaternary HPLC system equipped with a quaternary pump (G1312C), integrated degasser (G1322A), thermostatted column compartment (G1316A), autosampler (G1329B), diode-array detector (G1315D), and ChemStation software for data acquisition and analysis. We carried out chromatographic separation at 25 °C using a Pinnacle DB Silica column (5 µm, 4.6 × 250 mm; Restek) at a constant flow rate of 1.4 mL/min. For quantification, we calibrated the HPLC system with authentic standards of known carotenoids and retinoids. Peak areas were integrated to determine the concentration of each compound in the samples. We purchased all-*trans* retinol and retinal standards from Toronto Biochemicals. Carotenoid standards, including β-carotene, echinenone, canthaxanthin, and astaxanthin, were a gift from Dr. Adrian Wyss (DSM Ltd., Sisseln, Switzerland).

HCR for *bco1* and *bco1l* expression

We performed in situ hybridization chain reaction (HCR) to detect *bco1* and *bco1l* mRNA transcripts in wild-type betta larvae at 3, 5,

Downloaded from academic.oup.com/genetics/article/233/1/iyag049/8498880 by Columbia University Libraries user on 04 October 2026

and 10 dpf, using the standard protocol and reagents from Molecular Instruments (v3.0 protocol, Choi et al. 2018). We designed HCR probe sets following the method and code presented in (Kuehn et al. 2022), and probe sequences are available in Supplementary Table 1. We ordered probes as oPools Oligo Pools (IDT). We anesthetized fish in 0.8% MS-222 and euthanized them by immersion in ice-cold water. We fixed samples overnight at 4 °C in 4% paraformaldehyde (PFA) and then washed them 3 times in PBS. Samples were cryoprotected by stepwise incubation in 15% and 30% sucrose in PBS until they sank. We then embedded them in "optimal cutting temperature" (OCT) and stored them at −70 °C until use. We sectioned each sample at 7 μm thickness in the horizontal plane using a cryostat. We post-fixed the slides in 4% PFA for 15 min at 4 °C. Our remaining steps followed the protocol described in the HCR™ Gold RNA-FISH user guide. We included negative controls by processing samples identically but omitting the probe during hybridization. We imaged the samples using a W1-Yokogawa Spinning Disk Confocal microscope. We applied linear adjustments to brightness and contrast uniformly across images.

Conservation and evolution of *bco1* and *bco1l*

We determined that *bco1l* arose by duplication of *bco1* in the stem lineage of the ray-finned fishes (Actinopterygii) based on the following: (i) *bco1* is the most similar paralog of *bco1l* according to Ensembl release 114 (May 2025) Gene Tree (Dyer et al. 2025); (ii) *bco1l* and *bco1* are adjacent to each other in a head to tail orientation in the genomes of several ray-finned fishes that are not monophyletic (eg *Erpetoichthys calabaricus*, *D. rerio*, *Salmo salar*), and Genomicus v110.01 (Nguyen et al. 2022) places these 2 genes adjacent to each other in its reconstruction of the ancestral state of ray-finned fishes; and (iii) according to Ensembl, Genomicus, and NCBI Orthologs (Sayers et al. 2024), *bco1l* has orthologs in fish species from all Actinopterygii lineages (Cladistia, Chondrostei, Holostei, and Teleostei) but not in any non-Actinopterygii species; and (iv) according to Ensembl, Genomicus, and NCBI Orthologs, *bco1* is present throughout vertebrates.

To analyze the exon–intron structure of *bco1* (transcript variant X1) and *bco1l* (transcript variant X1), we obtained the lengths of the exons and introns for each gene from NCBI. We then aligned the mRNA transcripts from both genes using Clustal Omega (Ahmad et al. 2025) and determined homologous regions for each exon. We annotated indels in either gene if they exceeded 8 nucleotides in length. We then aligned the protein sequences of both genes using Clustal Omega and determined the percent identity along the lengths of the proteins in 20 amino acid windows with a step size of 5 amino acids.

Presence of *bco1* and *bco1l* across Actinopterygii

We obtained the list of all 222 unique ray-finned species with an annotated reference genome with a BUSCO total copy percentage >90% from NCBI (Sayers et al. 2024). We then checked whether NCBI had identified putative orthologs for *bco1* and/or *bco1l* for every species in the list. If an ortholog was identified, we listed that species as having that gene. In the remaining species for which NCBI did not identify and ortholog for one or both genes, we searched for the missing ortholog using the following steps: (i) We checked the Ensembl comparative genomics (release 113) database (Dyer et al. 2025) by searching for the gene name (*bco1* or *bco1l*) and the species or by locating the Ensembl gene in the NCBI genome data viewer; (ii) we manually searched for the missing orthologs in the species' NCBI reference genome using BLASTp and reciprocal best match with the betta *bco1* and *bco1l* amino acid sequences (Ward and Moreno-Hagelsieb 2014); (iii) we checked for orthologs using BLASTp in any alternative annotated reference genomes for those species available from NCBI.

For species in which we failed to identify orthologs for one of the 2 genes using these methods, we blasted the *bco1* or *bco1l* nucleotide sequence (discontiguous megablast) of the most closely related species included in our analysis against any unannotated alternative reference genomes available from NCBI. If we found a significant hit, we individually blasted the nucleotide sequence of each exon in the gene of the closely related species against the species being analyzed and constructed the mRNA sequence of the missing gene. We then established an open reading frame by aligning the 2 mRNA sequences (that of the species being analyzed and their close relative) using Clustal Omega. We translated the mRNA sequence and checked for premature stop codons. Finally, we blasted the amino acid sequence of the newly annotated gene against the betta genome using BLASTp to ensure that the top hit was the expected gene. We identified *bco1* orthologs in *Poecilia mexicana*, *Poecilia latipinna*, and *Poecilia formosa* as well as a *bco1l* ortholog in *Salarias fasciatus* using this method.

We failed to identify an ortholog for *bco1l* in *Notolabrus celidotus*, *Gymnodraco acuticeps*, *Etheostoma spectabile*, and *Pseudochaenichthys georgianus*. For these species, we blasted the nucleotide sequence of genes from 2 closely related species in the genomic vicinity of *bco1l* to check for reference genome integrity in the syntenic region. However, we were unable to navigate to the syntenic region in any of these species, making it difficult to determine whether the lack of *bco1l* represented a true evolutionary loss or an incomplete genome assembly. All *bco1* and *bco1l* orthologs we identified are listed in Supplementary Table 2.

Statistical analyses

We performed all statistical tests in RStudio v.2024.12.1 (R v.4.4.3) (R Core Team 2025). When we log-transformed data for visualization, we performed statistical analyses on the transformed datasets. All reported fold-differences were calculated using back-transformed group means. All data represented in figures are available in Supplementary Table 3.

For the linear mixed model (LMM) for the length of fish through development, we included genotype, age, and genotype*age as fixed effects, with individual as the random effect. For the LMM for length in the RA treatment experiment, we included treatment/genotype, age, and treatment/genotype*age as fixed effects, with individual as the random effect. We determined the significance of fixed effects using a type III ANOVA with Satterthwaite's method and performed all pairwise comparisons using Tukey's HSD.

Results

bco1l is required for juvenile but not embryonic or early larval development

While the consequences of a lack of *bco1* have been studied in *Danio* fish and mice (Lampert et al. 2003; Hessel et al. 2007; Kim et al. 2011; Huang et al. 2021), those of a *bco1l* knockout have not been documented. Upon discovering that homozygosity of a *bco1l* knockout mutation (a frameshift leading to a premature stop codon that preserves only the first fourth of the *bco1l* protein) was lethal in betta (Palmiotti et al. 2023), we set out to characterize the phenotypic consequences of the mutation and to identify when in development the mutants were dying. We initially imaged and genotyped larvae from a heterozygous × heterozygous cross at 3, 6, 10, 12, and 20 days post fertilization (dpf). Genotype

Downloaded from academic.oup.com/genetics/article/233/1/iyag049/8498880 by Columbia University Libraries user on 04 October 2026

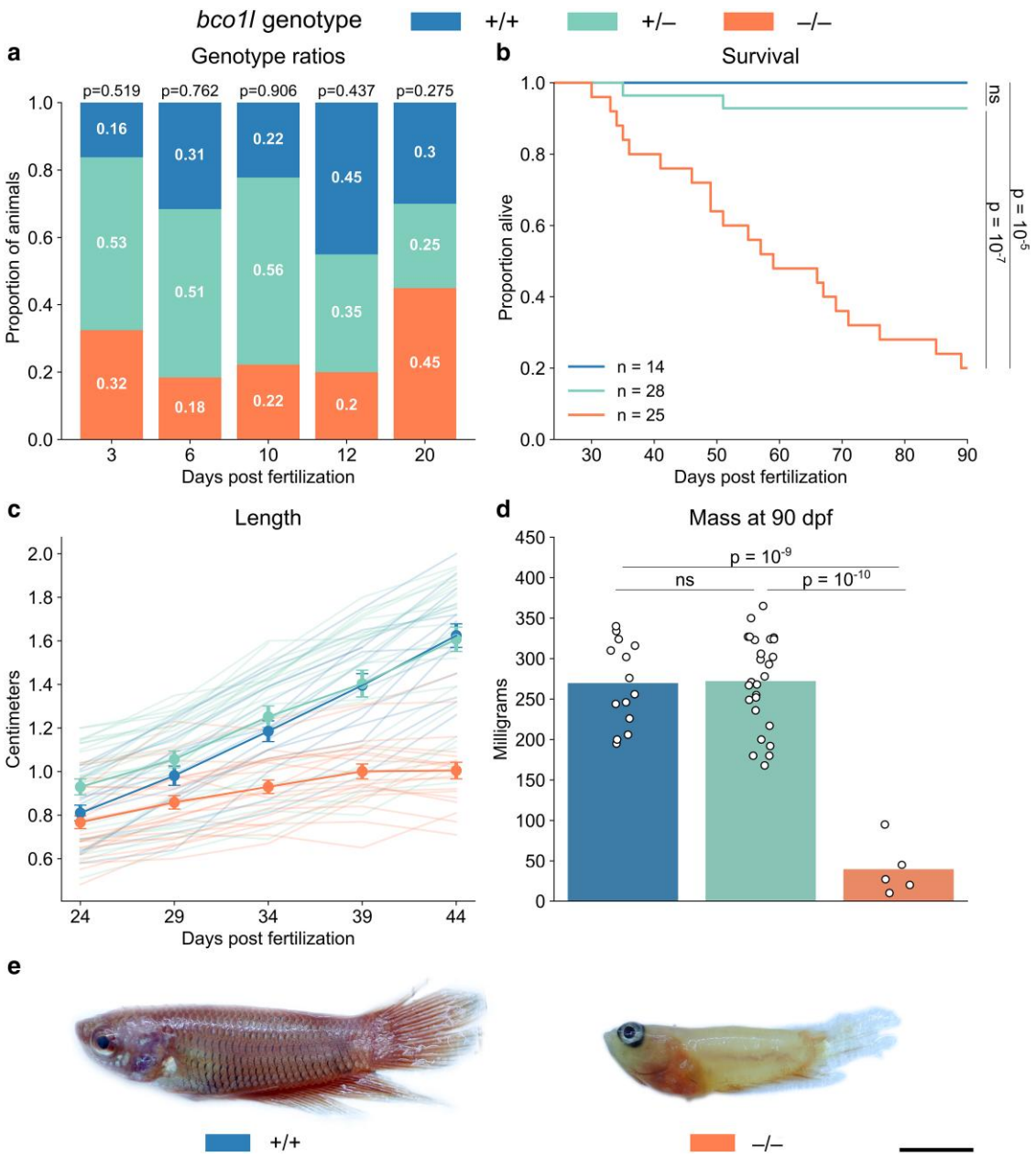

Fig. 2. *bco1l* is necessary for survival and growth in betta fish. a) Genotype ratios of fish sampled at 3, 6, 10, 12, and 20 days post fertilization (dpf) from a heterozygous cross. There was no significant deviation from the expected Mendelian ratios at any time point. *P*-values by Fisher's exact test. b) Survival curves for the three genotypes from 24 to 90 dpf. *P*-values by log-rank test adjusted by Bonferroni correction. c) Lengths of fish of the three genotypes from 24 to 44 dpf. Faint lines track the growth of individual fish; circles and whiskers denote the mean ± SEM. d) Masses of surviving fish of the three genotypes at 90 dpf. *P*-values by one-way ANOVA with Tukey's HSD. e) Representative images of +/+ and –/– individuals at 90 dpf. Scale bar: 5 mm.

ratios of the offspring did not differ significantly from the expected Mendelian ratios at any time point ($P > 0.05$, Fisher's exact tests; Fig. 2a), indicating that there was no mortality associated with the knockout up to 20 dpf. Furthermore, the knockouts appeared morphologically normal at all time points (Supplementary Fig. 1).

To determine at what age after 20 dpf the –/– fish were dying and to document their larval and juvenile development, we individually housed larval offspring from a heterozygous cross and measured growth and survival from 24 to 90 dpf. The –/– fish had impaired survival relative to both +/+ ($P = 10^{-5}$, Log-rank test adjusted by Bonferroni correction; Fig. 2b) and +/– fish ($P = 10^{-7}$). Mortality among the –/– individuals began at 30 dpf. At 90 dpf, only 20% of the original cohort were still alive. We note that when housed collectively, none of the –/– individuals survived to adulthood (Palmiotti et al. 2023). The improved survival (20%) of the –/– in this experiment might result from a lack of competition for food with their more robust +/+ and +/– siblings.

Genotype also had a significant effect on fish growth from 24 to 44 dpf ($P = 10^{-7}$, linear mixed model; Fig. 2c). The growth of the –/– fish was severely stunted: They were significantly shorter than the +/+ ($P = 0.039$, Tukey's HSD) and +/– ($P = 10^{-4}$) fish by 34 dpf and did not grow from 34 to 44 dpf ($P = 0.235$). By 90 dpf, the surviving –/– fish were 7-fold smaller by weight than the +/+ ($P = 10^{-9}$, one-way ANOVA with Tukey's HSD; Fig. 2d) and +/– ($P = 10^{-10}$) fish. The –/– individuals were also paler, did not properly develop scales,

Downloaded from academic.oup.com/genetics/article/233/1/iyag049/8498880 by Columbia University Libraries user on 04 October 2026

and exhibited erratic swimming behavior (Fig. 2e; Supplementary Video 1). Altogether, these results demonstrate that *bco1l* is essential for growth and survival during juvenile development in betta.

bco1l knockouts are retinoic acid deficient

After documenting the time of death and altered morphology of −/− animals, we sought to characterize the biochemical consequences of the *bco1l* mutation. *bco1l* cleaves β-carotene into two molecules of retinal, which is then converted into retinoic acid (RA). RA is difficult to quantify directly due to its low physiological concentration, particularly when working with minuscule tissue samples (~1 mg). A useful proxy for RA levels is *cyp26a1*, which encodes an enzyme that degrades RA, is induced by RA, and correlates with RA concentrations (Isken et al. 2007, 2008; Hu et al. 2008; Samarut et al. 2015). To test for evidence of altered RA levels in our *bco1l* mutants, we used digital PCR for absolute quantification of *cyp26a1* mRNA. There was no difference in *cyp26a1* expression between +/+, +/−, and −/− fish at 3 dpf, which is one day after hatching ($P = 0.176$, one-way ANOVA; Fig. 3a), suggesting that RA levels were equivalent among the genotypes and that *bco1l* is not required for RA production prior to 3 dpf. By 10 dpf, however, the −/− larvae had 6-fold lower *cyp26a1* than both the +/+ ($P = 10^{-6}$, one-way ANOVA with Tukey's HSD) and +/− individuals ($P = 10^{-8}$), while +/+ and +/− did not differ in *cyp26a1* expression ($P = 0.998$). The same pattern was apparent at 20 dpf, with the −/− larvae having reduced *cyp26a1* expression relative to both the +/+ ($P = 0.035$) and +/− ($P = 0.015$) individuals. This pattern of expression across genotypes suggests that *bco1l* is required for RA production during larval, but not embryonic, development in betta.

In addition to β-carotene, ketocarotenoids have pro-VA activity in fish (Schiedt et al. 1985; Kaisuyama and Matsuno 1988; Yamashita et al. 1996; Moren et al. 2002). To confirm that the reduced RA levels were due to the inability of the −/− larvae to convert β-carotene to VA, we quantified β-carotene, ketocarotenoids, and retinol in 20 dpf larvae of the three genotypes using high-performance liquid chromatography (HPLC) (Fig. 3, b and c). The concentration of β-carotene in +/− individuals was approximately twice that in +/+, demonstrating the system's dosage-sensitivity to *bco1l* with regards to β-carotene metabolism ($P = 0.003$, Welch's *t*-test adjusted by Bonferroni correction; Fig. 3c). Furthermore, the −/− larvae displayed a mean concentration of β-carotene 25× higher than that of +/+ larvae ($P = 10^{-5}$). We found no significant difference in ketocarotenoid or retinol content across the 3 genotypes, though we note that the −/− larvae had 1.8× less retinol than +/+. Retinyl esters were not detected in the −/− larvae but were present in both the +/+ and +/− individuals (Fig. 3b). Altogether, the accumulation of β-carotene and the reduction of retinol and retinyl esters indicate that *bco1l* is necessary for VA production in larval betta, explaining the deficit of RA in homozygous *bco1l* mutant animals.

Retinoic acid partially rescues the *bco1l* mutation

Retinoic acid is a highly biologically active VA metabolite (Duester 2008; O'Byrne and Blaner 2013; Petkovich and Chambon 2022). To test for a causal relationship between the reduced RA levels in our knockouts and their stunted growth and death, we sought to rescue the −/− phenotype via exogenous RA supplementation. To that end, we housed larvae of the three genotypes in 5 nM RA (dissolved in a 0.1% DMSO solution) beginning at 5 dpf. This RA concentration is consistent with that of previous successful RA rescue experiments in developing zebrafish (Begemann et al. 2001; Wang et al. 2017). *bco1l* +/+ and +/− did not differ in their response to RA supplementation, so we combined these groups to increase our statistical power. In the control (DMSO only) group, expression of *cyp26a1* at 10 dpf in the +/+ plus +/− individuals was 12-fold higher than in the −/− larvae ($P = 10^{-6}$, Welch's *t*-test adjusted by Bonferroni correction; Fig. 4a), supporting our prior conclusion that −/− animals without RA supplementation have reduced RA levels (Fig. 3a). RA treatment increased *cyp26a1* expression in +/+ plus +/− ($P = 10^{-10}$) and in −/− ($P = 10^{-8}$) relative to their respective control groups, demonstrating that exogenous RA was likely absorbed by the larvae. Furthermore, when supplemented with RA, there was no significant difference in *cyp26a1* expression between the +/+ plus +/− group compared to −/− larvae ($P = 0.343$). This indicates that RA supplementation rescued the RA deficit and effectively equalized RA levels among fish of the three genotypes.

To assess the effect of RA treatment on growth and survival, we individually housed larvae with RA (dissolved in DMSO) or control (DMSO) from 15 to 60 dpf. RA significantly increased the survival of −/− fish ($P = 0.016$, Log-rank test adjusted by Bonferroni correction; Fig. 4b). Furthermore, there was no significant difference in survival on RA between the +/+ plus +/− group compared to −/− ($P = 0.324$), demonstrating that equalizing RA levels among genotypes equalized their survival. The +/+ plus +/− group on RA had increased mortality relative to their non-RA supplementation control ($P = 0.006$), which we attribute to toxicity of excessive RA (Chawla et al. 2018; Wang et al. 2023). Since the −/− fish had similar *cyp26a1* expression as the +/+ plus +/− group on RA, RA toxicity likely also prevented the full rescue of the −/− relative to the +/+ plus +/− controls. Altogether, these results suggest that −/− fish die due to RA deficiency. RA supplementation and genotype also had a significant effect on growth ($P = 10^{-8}$, linear mixed model; Fig. 4c). Control −/− individuals did not grow from 24 to 44 dpf ($P = 0.444$, Tukey's HSD), while −/− on RA grew significantly ($P = 10^{-12}$), demonstrating that RA treatment partially rescued growth. Furthermore, there was no significant difference in length between the +/+ plus +/− group on RA compared to −/− on RA at any time point ($P > 0.05$), and no difference in mass between these groups at 60 dpf ($P = 0.754$, Welch's *t*-test adjusted by Bonferroni correction; Fig. 4d), indicating that RA eliminated growth differences between genotypes. We observed no apparent morphological differences among animals of the different genotypes treated with RA (Fig. 4e). Consistent with a toxic effect of RA, +/+ plus +/− and −/− animals treated with RA were significantly shorter than the +/+ plus +/− controls by 44 dpf ($P = 10^{-13}$, $P = 10^{-6}$, Tukey's HSD) and weighed significantly less at 60 dpf ($P < 10^{-16}$, $P = 10^{-5}$, Welch's *t*-test adjusted by Bonferroni correction). The results demonstrate that RA supplementation partially rescues both survival and growth of the *bco1l* mutation, indicating that the deleterious effects of the knockout are due primarily to RA deficiency. This is consistent with previous studies showing that insufficient VA during fish larval development can cause both stunted growth and death (Hernandez and Hardy 2020).

Expression of *bco1* and *bco1l* and carotenoid metabolism during development

In addition to *bco1l*, *bco1* is also capable of catalyzing the conversion of β-carotene to retinal in ray-finned fish species (Lampert et al. 2003). In Sarcopterygii species such as humans and rats, β-carotene conversion in the intestinal mucosa via *bco1* produces retinoids for system-wide regulation of apoptosis, immunity, and metabolism, processes essential for survival and growth (Lindqvist and Andersson 2002, 2004; von Lintig et al. 2005; Takitani et al. 2006; Noy 2010; Raverdeau and Mills 2014). To investigate why *bco1* does not compensate for the lack of *bco1l* in betta

Downloaded from academic.oup.com/genetics/article/233/1/iyag049/8498880 by Columbia University Libraries user on 04 October 2026

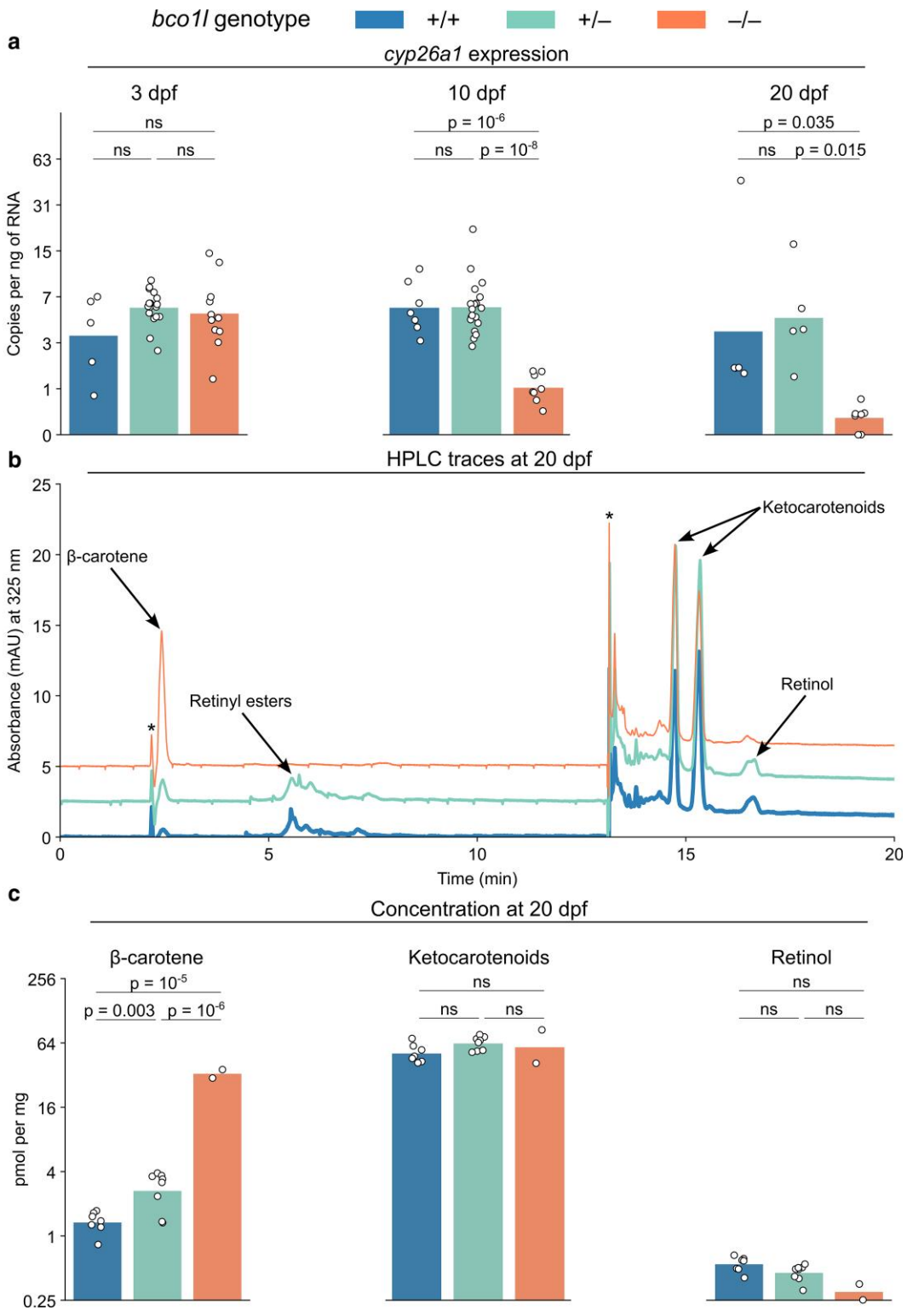

Fig. 3. *bco1l* is essential for β-carotene conversion to vitamin A in larval betta fish. a) Whole-body *cyp26a1* expression at 3, 10, and 20 days post fertilization (dpf) across *bco1l* genotypes. P-values by one-way ANOVA with Tukey's HSD. b) HPLC chromatograms across *bco1l* genotypes. Peaks corresponding to β-carotene, retinyl esters, ketocarotenoids, and retinol are indicated. * denotes peaks arising from a gradient solvent composition change. The +/– and –/– traces are vertically offset by 2.5 and 5 mAU, respectively, for ease of visualization. c) β-carotene, ketocarotenoid, and retinol concentrations in 20 dpf larvae of the three genotypes. P-values by Welch's t-test adjusted by Bonferroni correction.

and to better understand how *bco1l* controls VA production, we characterized the expression levels and patterns of the two genes throughout development. Both *bco1* and *bco1l* were expressed in the intestine of betta larvae at 3, 5, and 10 dpf (Fig. 5a). At 3 dpf, *bco1* and *bco1l* expression overlapped in the intestinal epithelium. This pattern remained at 5 dpf, with both transcripts co-expressed

Downloaded from academic.oup.com/genetics/article/233/1/iyag049/8498880 by Columbia University Libraries user on 04 October 2026

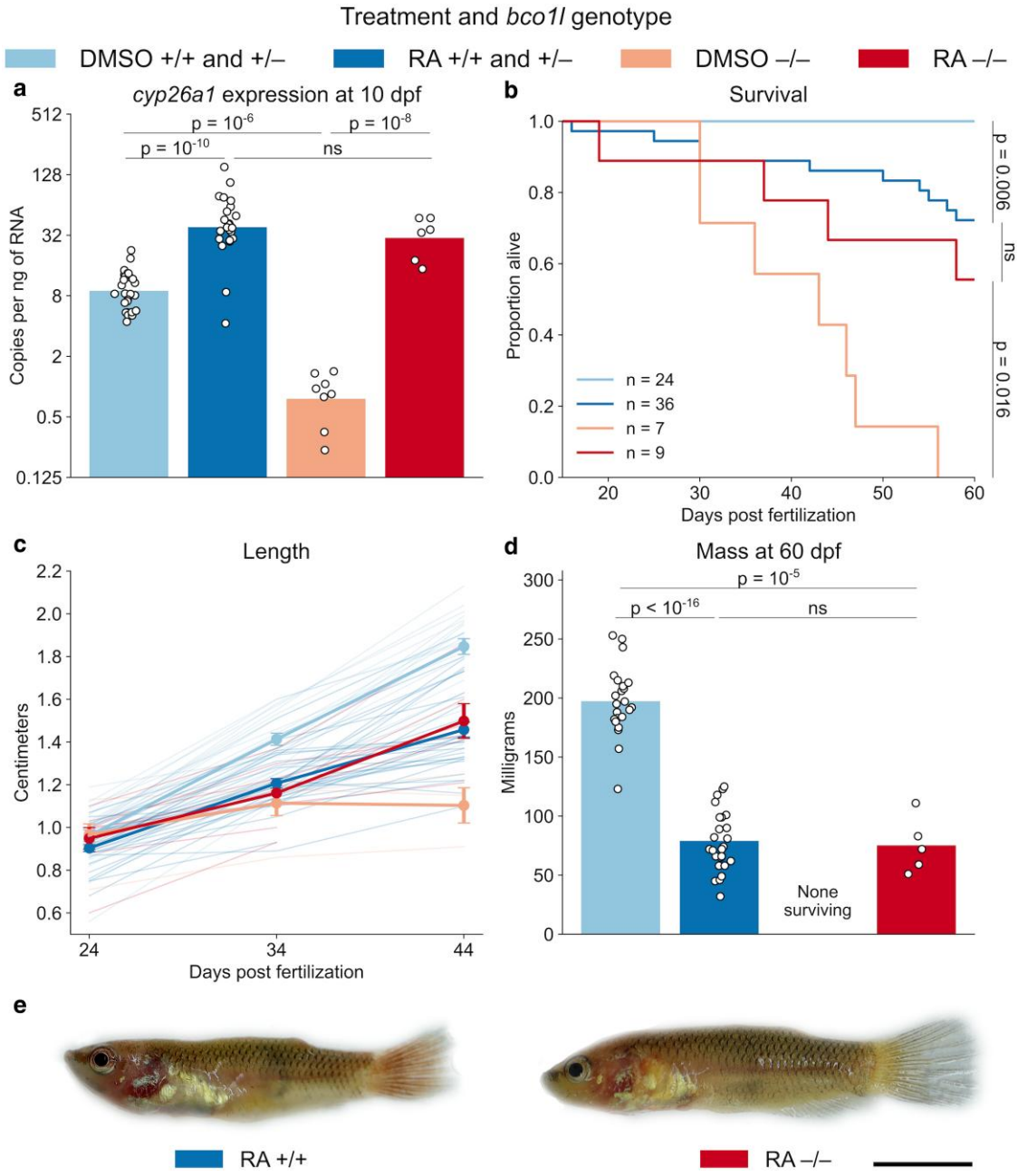

Fig. 4. Exogenous retinoic acid supplementation partially rescues the *bco1l* knockout phenotype. a) Whole-body *cyp26a1* expression in DMSO control and RA-treated cohorts of different genotypes at 10 days post fertilization (dpf). *P*-values by Welch's *t*-test adjusted by Bonferroni correction. b) Survival curves for DMSO control and RA-treated individuals from 15 to 60 dpf. *P*-values by log-rank test adjusted by Bonferroni correction. c) Lengths of –/– and +/+ plus +/– fish in the DMSO control and RA-treated groups at 24, 34, and 44 dpf. Faint lines denote the growth of individual animals, circles and whiskers denote the mean ± SEM. d) Masses at 60 dpf. *P*-values by Welch's *t*-test adjusted by Bonferroni correction. e) Representative images of RA-treated +/+ and –/– animals at 60 dpf. Scale bar: 5 mm.

in the developing intestine. By 10 dpf, co-expression of *bco1* and *bco1l* persisted in the intestine and was also detected in the liver. To measure the relative expression levels of the two genes in different tissues, we quantified absolute numbers of *bco1* and *bco1l* transcripts using digital PCR in various tissues in adult betta, when animals are large enough to facilitate the dissection of individual tissues. *bco1l* was 7-fold more abundant in the intestine than *bco1* ($P = 0.006$, two-sided paired *t*-test; Fig. 5b), consistent with the higher intestinal expression of *bco1l* observed in Atlantic salmon (Helgeland et al. 2014). *bco1* was 6-fold more abundant in skin ($P = 0.017$) and 2-fold more abundant in the eye ($P = 0.009$). The enriched skin expression is consistent with the effects of *bco1* mutation on skin pigment cells in zebrafish and pearl danio (Lampert et al. 2003; Huang et al. 2021). Both genes are expressed at similar levels in the gonads, head kidney, and liver. We did not detect expression of either paralog in muscle tissue, which contrasts with salmon, where both genes are expressed at low levels (Helgeland et al. 2014). Altogether, these results suggest that *bco1l* might be responsible for the bulk of β-carotene metabolism in the intestinal epithelium, where expression is detectable as early as 3 dpf and is higher than that of *bco1* in adults. By contrast, *bco1* activity may predominate in the eyes and skin.

Downloaded from academic.oup.com/genetics/article/233/1/iyag049/8498880 by Columbia University Libraries user on 04 October 2026

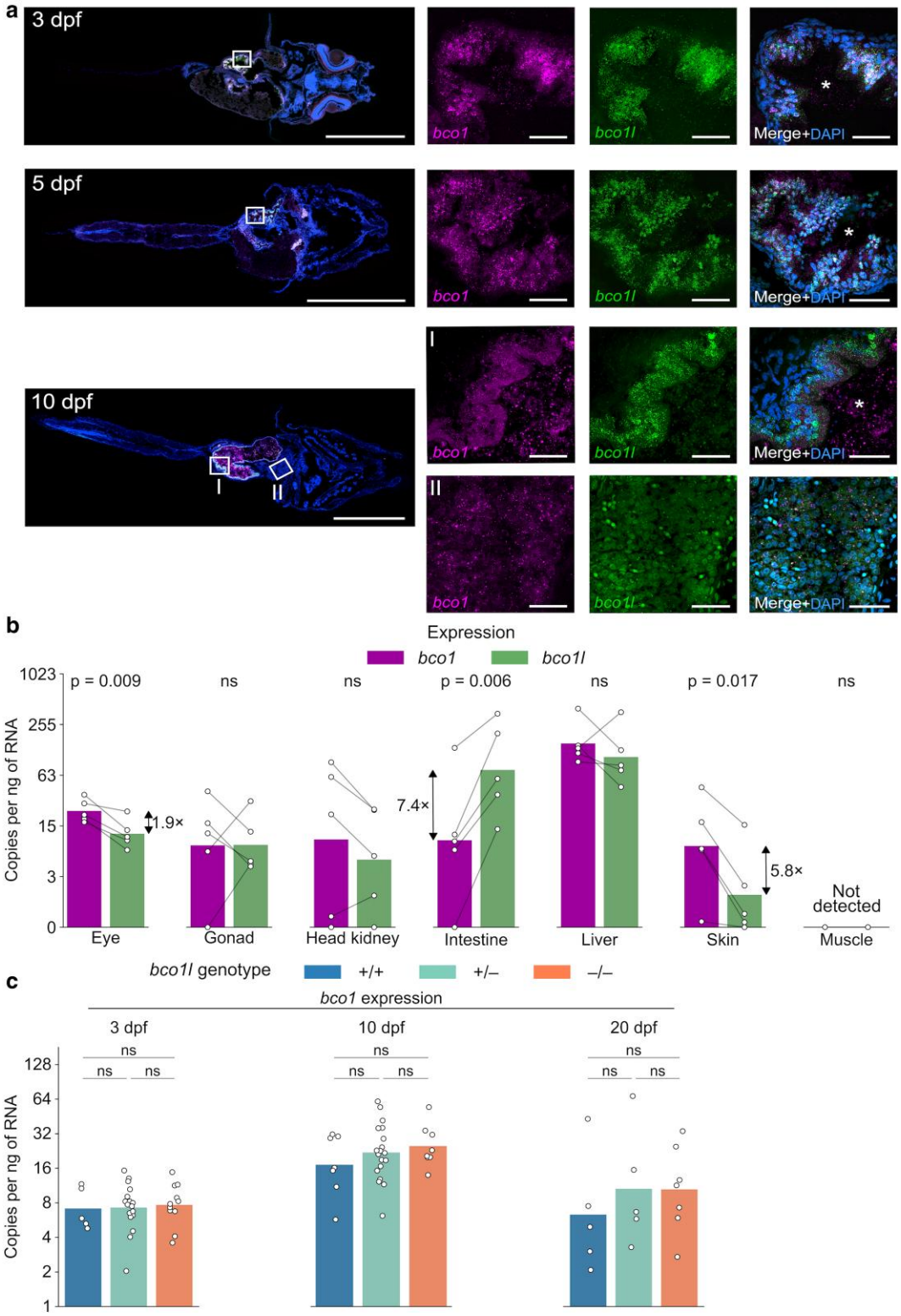

Fig. 5. Spatiotemporal expression of *bco1* and *bco1l*. a) Detection of *bco1* and *bco1l* transcripts in wild-type larvae using *in situ* hybridization chain reaction at 3, 5, and 10 days post fertilization (dpf). I. Inset from 10 dpf highlighting the intestine. II. Inset from 10 dpf highlighting the liver. * marks the intestinal lumen. Scale bars: 500 µm (whole larvae sections); 25 µm (magnified insets). b) Expression of *bco1* and *bco1l* in various tissues in adult betta. *P*-values by paired *t*-test. Data are paired by individual. c) Expression of *bco1* at 3, 10, and 20 dpf in *bco1l* knockouts. *P*-values by one-way ANOVA.

To test whether *bco1* expression is upregulated to compensate for the lack of *bco1l* in the knockouts, we quantified *bco1* expression at 3, 10, and 20 dpf in whole larvae (Fig. 5c). As expression of *bco1* is restricted to the intestine and liver during larval development (Fig. 5a), our results are likely indicative of transcript abundance in these tissues. There was no difference in *bco1* expression

Downloaded from academic.oup.com/genetics/article/233/1/iyag049/8498880 by Columbia University Libraries user on 04 October 2026

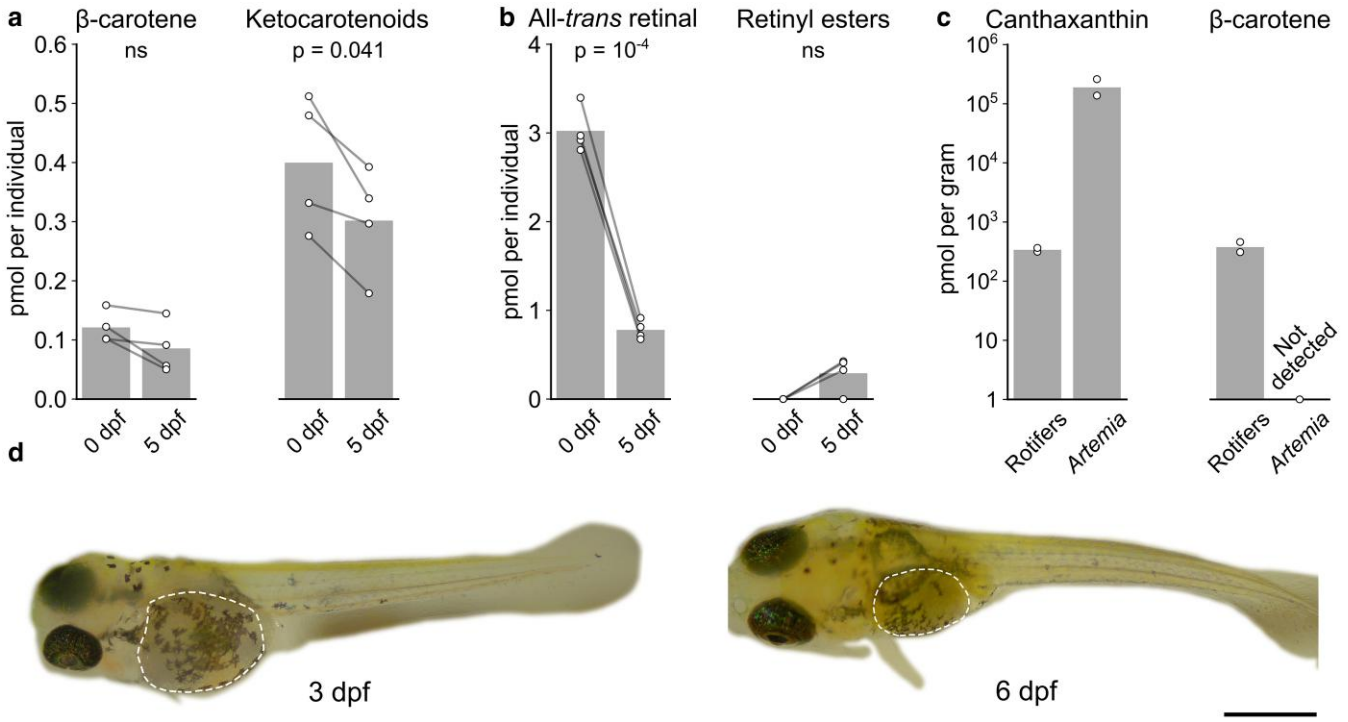

Fig. 6. Carotenoids and retinoids during betta development. a, b) Concentration of β-carotene and ketocarotenoids (a) and retinoids (b) in betta eggs and larvae at 5 days post fertilization (dpf). *P*-values by paired *t*-test. Data are paired by cross. c) Concentrations of canthaxanthin and β-carotene in samples of rotifer and newly hatched brine shrimp (*Artemia nauplii*) feeds. d) Representative images of 3 dpf and 6 dpf betta. Dashed lines mark the yolk sack, which shrinks substantially as it is consumed from 3 to 6 dpf. Scale bar: 1 mm.

among *bco1l* genotypes at any time point ($P = 0.937$, $P = 0.417$, $P = 0.667$, one-way ANOVAs). −/− fish are RA deficient at 10 and 20 dpf, and both +/− and −/− fish accumulate β-carotene by 20 dpf (Fig. 3). Therefore, this result demonstrates that *bco1* is not upregulated in response to insufficient RA or to increased β-carotene concentration in *bco1l* mutants.

RA is essential for pattern formation during embryonic development (Berenguer and Duester 2022). We therefore sought to characterize the generation and utilization of VA (the RA precursor) through embryonic development in betta and to determine why lack of *bco1l* expression does not appear to affect RA concentrations prior to 3 dpf but reduces them dramatically by 10 dpf (Fig. 3a). We used HPLC to separate β-carotene, ketocarotenoids, and retinoids in eggs and 5 dpf larvae (before they start food intake) of developing betta (Supplementary Fig. 2). There was no significant difference in β-carotene concentration between eggs and 5 dpf larvae ($P = 0.083$, two-sided paired *t*-test; Fig. 6a) while total ketocarotenoid content was ~25% lower in the 5 dpf larvae than the eggs ($P = 0.041$). This suggests that only small amounts of yolk β-carotene and ketocarotenoids are used for VA synthesis during embryonic and early larval development. To test whether betta embryos and larvae may use retinoids stored in the yolk, we also measured all-*trans* retinal and retinyl ester levels. The concentration of all-*trans* retinal in eggs was 7.5 to 25× higher than that of ketocarotenoids and β-carotene. By 5 dpf, the all-*trans* retinal concentration had decreased by 74% ($P = 10^{-4}$; Fig. 6b). Retinyl esters were not detected in eggs (Fig. 6b; Supplementary Fig. 2a), suggesting that betta, like other fish, store maternal VA as retinal bound to vitellogenin (Irie and Seki 2002; Lampert et al. 2003). Retinyl esters increased slightly by 5 dpf in some animals, indicating a portion of this retinal is converted to retinyl esters by that time (Fig. 6b; Supplementary Fig. 2b). The much lower levels of carotenoids compared to all-*trans* retinal in the eggs, coupled with a reduction in all-*trans* retinal through development to 5 dpf, suggest that larvae do not use yolk carotenoids as a significant source for retinoid production by 5 dpf and instead use all-*trans* retinal stored in the yolk.

As vertebrates obtain pro-VA carotenoids and/or VA retinoids from food throughout life, we also determined the pro-VA carotenoid content in rotifers, which we feed betta fish from 5 to 14 dpf, and in newly hatched brine shrimp (*Artemia nauplii*), which we feed betta from 15 dpf onwards. In rotifers, we identified a major chromatographic peak as β-carotene based on its retention time and spectral profile (Supplementary Fig. 2e). We did not detect β-carotene in *Artemia* (Fig. 6c; Supplementary Fig. 2f). Both rotifers and *Artemia* contained canthaxanthin and an additional unidentified ketocarotenoid. Additional peaks did not match the spectral properties of known carotenoids or retinoids. Our results indicate that betta larvae have access to dietary β-carotene and ketocarotenoids after 5 dpf (when they start eating rotifers). We suggest that the intestinal conversion of β-carotene and ketocarotenoids (likely converted into β-carotene first by other enzymes; Fig. 1) to retinal by *bco1l* becomes critical after this point as they are exhausting their yolk stores of VA. This explains the reduced *cyp26a1* expression in the 10 and 20 dpf *bco1l* knockouts.

Evolution and conservation of *bco1* and *bco1l*

While one of a pair of paralogous genes is typically pseudogenized (Lynch and Conery 2000), *bco1* and *bco1l* are found across ray-finned fishes (Helgeland et al. 2014). Our identification of an essential function for *bco1l* in VA production and the differences in expression between *bco1* and *bco1l* prompted us to investigate the emergence of *bco1l* in the phylogenetic history of vertebrates.

Downloaded from academic.oup.com/genetics/article/233/1/iyag049/8498880 by Columbia University Libraries user on 04 October 2026

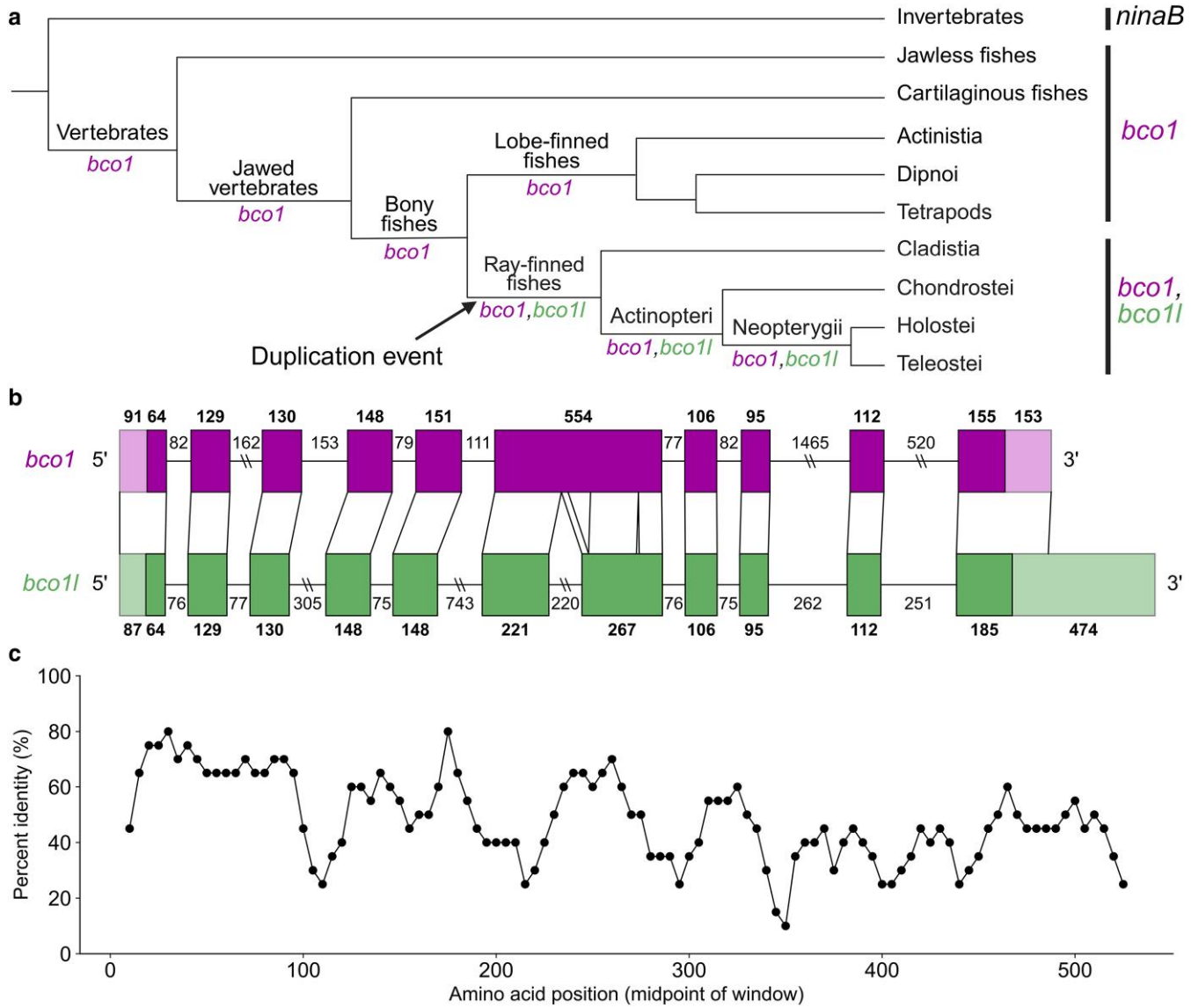

Fig. 7. *bco1l* emerged from a duplication event in the stem lineage of ray-finned fishes. a) Vertebrate phylogeny showing the presence of *bco1* and *bco1l* across lineages. *ninaB* is the invertebrate homolog. b) Exon–intron structure of betta *bco1* and *bco1l*. Lines connecting exons between the 2 genes indicate homologous regions. c) Percent identity of betta *bco1* and *bco1l* proteins. Points denote the percent identity of 20 amino acid windows with a 5 amino acid slide. The overall percent identity between the proteins is 47.7%.

ninaB is the invertebrate ortholog to *bco1* and *bco1l* and acts as a carotenoid oxygenase (von Lintig and Vogt 2000). It also acts as a retinoid isomerase, a function performed by *rpe65* in vertebrates (Oberhauser et al. 2008). We found *bco1* in all major vertebrate taxa, but *bco1l* was restricted to ray-finned fishes (Fig. 7a).

Next, we probed the evolutionary origin of *bco1l* in more detail. If *bco1l* had arisen through a retrotransposition event, it would have no introns. However, the exon–intron structure of *bco1l* is conserved with *bco1* (Fig. 7b). Furthermore, ancestral state reconstructions place *bco1* and *bco1l* adjacent to each other at the base of ray-finned fishes (see Methods). A parsimonious explanation for these observations, along with the phylogenetic pattern, is that *bco1l* emerged through a segmental duplication event in the stem lineage of the ray-finned fishes (Fig. 7a). Alignment of the amino acid sequences of betta *bco1* (547 residues) and *bco1l* (534 residues) revealed similarity across the lengths of the proteins, with an overall percent identity of 47.7% (Fig. 7c). This indicates that the duplication included the entirety of the ancestral *bco1* protein, and that no particular region has diverged more than others.

While both *bco1* and *bco1l* have been identified in numerous fish species, an inclusive analysis of their conservation across Actinopterygii taxa has not been conducted. To determine the evolutionary persistence of *bco1* and *bco1l*, we looked for evidence of each gene in 222 Actinopterygii species using publicly available reference genomes. To minimize false negatives, we excluded species for which one of the genes was not identified that had reference genomes with a BUSCO total copy percentage lower than 90%. We identified *bco1* orthologs in all analyzed species and *bco1l* orthologs in 218 of 222 (Supplementary Table 2). We failed to identify *bco1l* in the following 4 species: *E. spectabile*, *G. acuticeps*, *N. celidotus*, and *P. georgianus*. However, it is unclear whether this represents true evolutionary losses or errors in the reference genome assemblies (see Materials and methods). Overall, our analysis demonstrates that both *bco1* and *bco1l* have been preserved throughout the ray-finned fishes.

Downloaded from academic.oup.com/genetics/article/233/1/iyag049/8498880 by Columbia University Libraries user on 04 October 2026

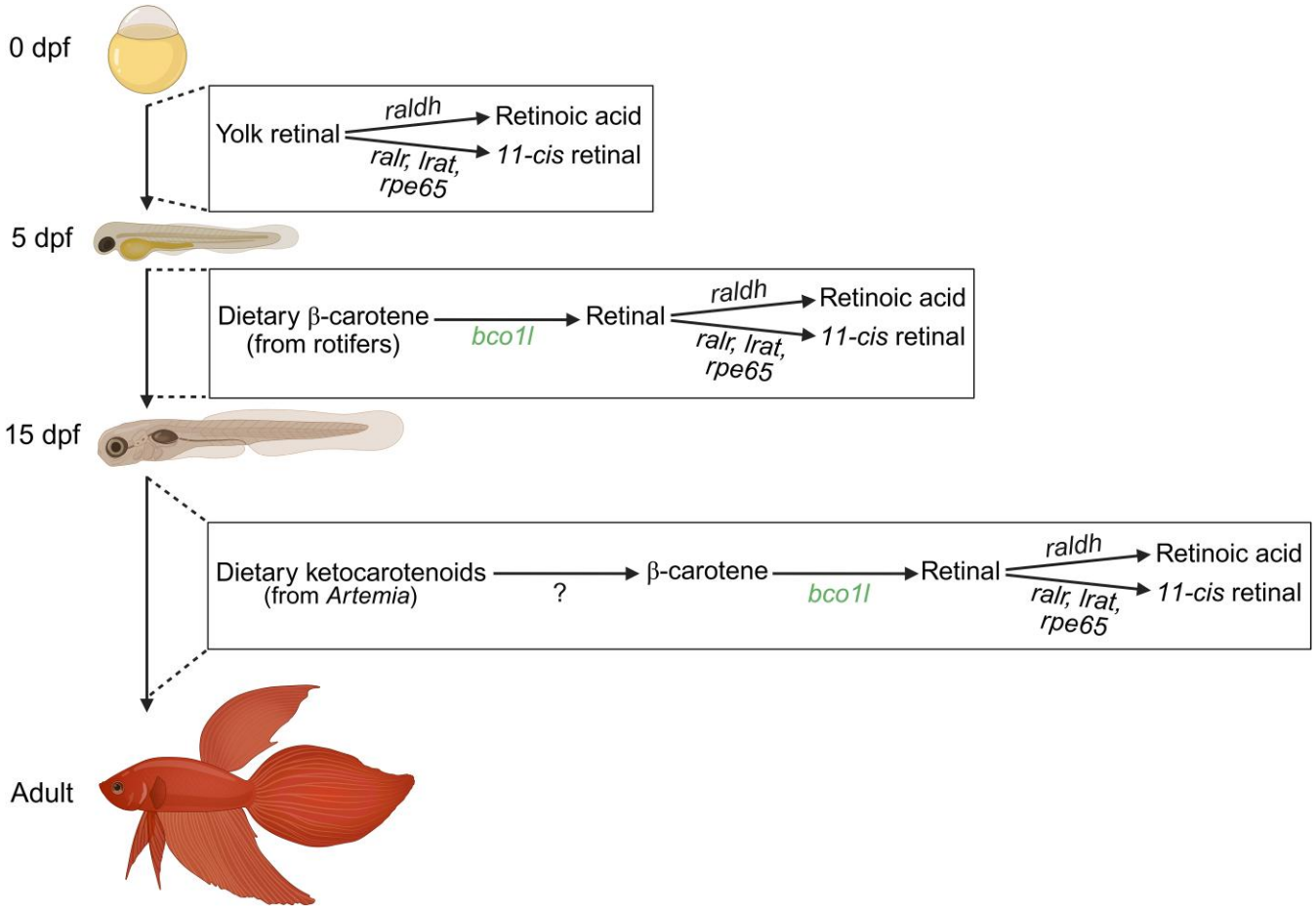

Fig. 8. Vitamin A production during betta development. From 0 to 5 days post fertilization (dpf), maternally deposited retinal in the yolk is utilized to produce the essential metabolite retinoic acid and the visual chromophore (*11-cis* retinal). Once the yolk stores of retinal are depleted, animals transition to retinoid production through the metabolism of dietary carotenoids. From 5 to 15 dpf, betta convert β-carotene from rotifer feeds to retinal via the 15,15′ oxygenase activity of *bco1l*. From 15 dpf to adulthood, betta rely on the provitamin A ketocarotenoid content of *Artemia* feeds. These ketocarotenoids are likely converted first to β-carotene and subsequently cleaved by *bco1l*. Created in BioRender.

Discussion

A model for vitamin A production via *bco1l* during development

By knocking out *bco1l* in betta fish, we discover that it is essential for VA and RA production. Lack of *bco1l* leads to stunted growth and death during development primarily due to insufficient RA. RA deficiency manifests after larvae have utilized the all-*trans* retinal stores in the yolk, the majority of which is likely used to support the development of photoreceptors in the eyes (Lampert et al. 2003; Isken et al. 2007). At this stage, larvae transition to metabolism of dietary pro-VA carotenoids for continued retinoid biosynthesis, and this metabolism requires *bco1l* (Fig. 8). Food sources rich in preformed VA may facilitate larval survival, yet the conservation of *bco1l* throughout ray-finned species suggests this gene has an essential role in nature.

In addition to β-carotene, ketocarotenoids including canthaxanthin are known to have pro-VA activity in fish (Schiedt et al. 1985; Kaisuyama and Matsuno 1988; Yamashita et al. 1996; Moren et al. 2002). Consistent with pro-VA activity of ketocarotenoids, wild-type betta showed no obvious signs of VA deficiency on a diet of *Artemia*, which contains canthaxanthin but no β-carotene nor preformed retinoids (Moren et al. 2005). By contrast, betta without *bco1l* are RA deficient and do not survive under this dietary condition. We therefore suggest that betta can convert ketocarotenoids to retinoids, and that this pathway involves the *bco1l* gene function. It is possible that *bco1l* directly cleaves ketocarotenoids to keto-retinoids, and that these compounds have VA activity. However, we found no biochemical evidence for ketocarotenoid cleavage by *bco1l* (unpublished observations), in contrast to its ability to cleave β-carotene (Helgeland et al. 2019; Kwon et al. 2022). We also observe accumulation of β-carotene, but not ketocarotenoids, in 20 dpf *bco1l* knockouts, indicating that the pathway is impeded at the level of β-carotene to retinal. Therefore, ketocarotenoids are likely first converted to β-carotene and then cleaved to canonical retinoids (Fig. 8), a pathway described in several other fish species (Schiedt et al. 1985; Kaisuyama and Matsuno 1988; Yamashita et al. 1996) and in VA-deficient rats (Sangeetha and Baskaran 2010).

Mechanisms underlying the *bco1l* knockout phenotype

RA acts as a ligand for nuclear receptors (RARs), exerting transcriptional control over a variety of target genes. During embryonic development, a spatiotemporal RA gradient is established via the production of RA and its enzymatic degradation across different cell types, controlling anteroposterior patterning, limb initiation, heart development, and eye morphogenesis (Begemann et al. 2001; Grandel et al. 2002; Keegan et al. 2005; Sandell et al.

Downloaded from academic.oup.com/genetics/article/233/1/iyag049/8498880 by Columbia University Libraries user on 04 October 2026

2007; Cunningham et al. 2013; Cunningham and Duester 2015; Berenguer et al. 2018; Berenguer and Duester 2022). As a result, disrupted RA signaling in embryonic zebrafish results in a curved body axis, malformed pectoral fins, cardiac edema, and microphthalmia (Begemann et al. 2001; Lampert et al. 2003; Isken et al. 2008; Le et al. 2012; D'Aniello et al. 2015). The absence of these defects in *bco1l* knockouts is consistent with the normal retinoid levels in wild-type and mutant betta during embryonic development. However, RA signaling is also important later in life, regulating apoptosis, osteoblast and osteoclast function, and immunity (Noy 2010; Raverdeau and Mills 2014; Green et al. 2016; Chawla et al. 2018). Our rescue experiments demonstrated that *bco1l* knockout phenotypes are caused by RA deficiency during larval and juvenile development, since treatment with exogenous RA improved survival.

Deposition of carotenoids into eggs varies across fish species

Consistent with our results in betta, zebrafish eggs contain retinal, β-carotene, and various ketocarotenoids (Lampert et al. 2003). By contrast, Chinook salmon (*Oncorhynchus tshawytscha*) eggs contain little β-carotene but high concentrations of the ketocarotenoid astaxanthin (Li et al. 2005), which decline substantially during early development (Tyndale et al. 2008). The eggs of another salmonid, brown trout (*Salmo trutta*), contain relatively little astaxanthin and more lutein and zeaxanthin than Chinook salmon, though still little to no β-carotene (Wilkins et al. 2017). Thus, pro-VA carotenoid deposition in egg yolk is rather variable. Differences in the amount and variety of carotenoids and retinoids available during embryonic development could influence RA production and the role of *bco1l* across species.

Evolution and functions of *bco1* and *bco1l*

Our phylogenetic analyses indicate that *bco1l* emerged via a gene duplication event in the stem lineage of the ray-finned fishes, updating prior interpretations of the origins of the *bco1* gene family (Helgeland et al. 2014). One of a pair of paralogous genes is usually pseudogenized shortly following duplication (Lynch and Conery 2000). This is particularly true in cases of small-scale duplication, as it often disrupts the balance of interacting gene products, resulting in deleterious effects that drive the nonfunctionalization of one of the paralogs (Birchler and Veitia 2012; Wilson and Liberles 2023). Nonetheless, we find both *bco1* and *bco1l* to be highly conserved across Actinopterygii, representing a useful case study for the evolution and preservation of duplicate genes.

Our *bco1l* knockout in betta provides insight into the relative function of *bco1* and *bco1l*. While both enzymes have been shown to cleave β-carotene in teleosts (Lampert et al. 2003; Helgeland et al. 2019; Kwon et al. 2022), VA deficiency in *bco1l* mutant fish is not compensated for by *bco1*, indicating that the two genes are not functionally redundant. In Sarcopterygii species, including humans, *bco1* converts the majority of dietary pro-VA carotenoids to retinoids in the intestinal mucosa (Lindqvist and Andersson 2002; Takitani et al. 2006). These compounds are then transported to the liver, from where they can be distributed through the blood to other tissues (Lindqvist and Andersson 2004; von Lintig et al. 2005; von Lintig 2010). While both *bco1* and *bco1l* are expressed in the intestine of developing betta, *bco1l* is 7× more abundant in the intestine of adult fish than *bco1*, consistent with the expression pattern observed in Atlantic salmon (Helgeland et al. 2014). Furthermore, *bco1* expression is not upregulated in the VA-deficient *bco1l* knockouts, contrasting with the upregulation of intestinal *bco1* expression in VA-deficient rats (Takitani et al. 2006). Finally, *bco1l* mutants accumulate β-carotene. Altogether, these results suggest that the relatively low intestinal *bco1* expression in betta is insufficient to compensate for the lack of *bco1l* and that *bco1l* may be primarily responsible for the intestinal conversion of carotenoids to VA in ray-finned fishes.

In addition to its role in the intestinal processing of carotenoids, mammalian *bco1* is expressed in various organs including kidney, eye, and lung, where it is thought to act in the local synthesis of retinoids (Paik et al. 2001; Yan et al. 2001; Lindqvist and Andersson 2004). In zebrafish, *bco1* is expressed in a distally enriched gradient in the caudal fin (Rabinowitz et al. 2017), and morpholino-mediated knockdown of the gene has cell-type-specific effects (Lampert et al. 2003), providing further support for localized retinoid biosynthesis by *bco1*. Consistent with this, we observe *bco1* expression in various tissues in adult betta, with higher expression than *bco1l* in the skin and eyes. The tissue-specific synthesis of retinoids by *bco1* has been implicated in embryonic development in several species, including zebrafish (Lampert et al. 2003; Mora et al. 2004; Kim et al. 2011). A potential model for the subfunctionalization of these twp genes relative to the ancestral *bco1* might therefore resemble the following: *bco1* acts to provide a local source of VA to tissues, such as those containing cells derived from the neural crest, while *bco1l* generates VA in bulk for storage and mobilization through its expression in the intestinal epithelium. This is consistent with the apparently normal embryonic development of betta *bco1l* knockouts and their manifestation of RA deficiency only following the switch to reliance on dietary carotenoids.

We note that the function of *bco1* in embryonic development in zebrafish has only been tested using morpholino-mediated knockdown, which has potential off-target effects (Lampert et al. 2003). In pearl danio, a close relative of zebrafish, a *bco1* loss-of-function mutation only leads to a subtle fin-pigmentation phenotype in adults due to reduced carotenoid concentrations in pigment cells, with no reported deficits in viability or fertility (Huang et al. 2021). The observed reduction in carotenoid levels is contrary to the expected accumulation due to a lack of *bco1* β-carotene oxygenase activity, warranting further investigation. Further developmental and biochemical studies of *bco1* and *bco1l* in betta and other ray-finned fishes are needed to fully elucidate their functions.

Conclusions

Our findings suggest that the conversion of dietary pro-VA carotenoids to retinal via *bco1l* is essential for retinoic acid-dependent processes in larval and juvenile betta fish. Our results demonstrate that *bco1l* is not redundant with *bco1* and that it has been preserved in the genomes of ray-finned fishes since its emergence in their stem lineage.

Data availability

The data underlying this article are available in the article and in its online Supplementary material.

Supplemental material available at GENETICS online.

Acknowledgments

Pei-Yin Shih provided technical assistance. Sam Szalkowski and Sebastian Lumapas helped with fish care and experiments.

Funding

This work was supported by the following grants: National Institutes of Health (NIH) R35GM143051 to A.B. and National

Downloaded from academic.oup.com/genetics/article/233/1/iyag049/8498880 by Columbia University Libraries user on 04 October 2026

Institutes of Health grants EY020551 and EY028121 to J.v.L. L.S.K received funding support from the Columbia University SURF program.

Conflicts of interest

None declared.

Author contributions

L.S.K., A.P., J.v.L, and A.B conceived the study. L.S.K., P.R.V., S.B., and Y.Z. performed experiments. L.S.K and P.R.V analyzed data and produced figures. L.S.K, P.R.V, and A.B. wrote the paper with revisions from all authors. J.v.L. and A.B. provided funding and resources.

Literature cited

Ahmad S *et al.* 2025. The UniProt website API: facilitating programmatic access to protein knowledge. Nucleic Acids Res. 53: W547–W553. https://doi.org/10.1093/nar/gkaf394.

Begemann G *et al.* 2001. The zebrafish *neckless* mutation reveals a requirement for *raldh2* in mesodermal signals that pattern the hindbrain. Development. 128:3081–3094. https://doi.org/10.1242/dev.128.16.3081.

Berenguer M *et al.* 2018. Mouse but not zebrafish requires retinoic acid for control of neuromesodermal progenitors and body axis extension. Dev Biol. 441:127–131. https://doi.org/10.1016/j.ydbio.2018.06.019.

Berenguer M, Duester G. 2022. Retinoic acid, RARs and early development. J Mol Endocrinol. 69:T59–T67. https://doi.org/10.1530/JME-22-0041.

Birchler JA, Veitia RA. 2012. Gene balance hypothesis: connecting issues of dosage sensitivity across biological disciplines. Proc Natl Acad Sci U S A. 109:14746–14753. https://doi.org/10.1073/pnas.1207726109.

Chawla B, Swain W, Williams AL, Bohnsack BL. 2018. Retinoic acid maintains function of neural crest–derived ocular and craniofacial structures in adult zebrafish. Invest Ophthalmol Vis Sci. 59: 1924–1935. https://doi.org/10.1167/iovs.17-22845.

Choi HMT *et al.* 2018. Third-generation *in situ* hybridization chain reaction: multiplexed, quantitative, sensitive, versatile, robust. Development. 145:dev165753. https://doi.org/10.1242/dev.165753.

Clagett-Dame M, DeLuca HF. 2002. The role of vitamin A in mammalian reproduction and embryonic development. Annu Rev Nutr. 22: 347–381. https://doi.org/10.1146/annurev.nutr.22.010402.102745E.

Cunningham TJ *et al.* 2013. Antagonism between retinoic acid and fibroblast growth factor signaling during limb development. Cell Rep. 3:1503–1511. https://doi.org/10.1016/j.celrep.2013.03.036.

Cunningham TJ, Duester G. 2015. Mechanisms of retinoic acid signalling and its roles in organ and limb development. Nat Rev Mol Cell Biol. 16:110–123. https://doi.org/10.1038/nrm3932.

D'Aniello E, Ravisankar P, Waxman JS. 2015. Rdh10a provides a conserved critical step in the synthesis of retinoic acid during zebrafish embryogenesis. PLoS One. 10:e0138588. https://doi.org/10.1371/journal.pone.0138588.

Duester G. 2008. Retinoic acid synthesis and signaling during early organogenesis. Cell. 134:921–931. https://doi.org/10.1016/j.cell.2008.09.002.

Dyer SC *et al.* 2025. Ensembl 2025. Nucleic Acids Res. 53:D948–D957. https://doi.org/10.1093/nar/gkae1071.

Goodman DS, Huang HS. 1965. Biosynthesis of vitamin A with rat intestinal enzymes. Science. 149:879–880. https://doi.org/10.1126/science.149.3686.879.

Grandel H *et al.* 2002. Retinoic acid signalling in the zebrafish embryo is necessary during pre-segmentation stages to pattern the anterior-posterior axis of the CNS and to induce a pectoral fin bud. Development. 129:2851–2865. https://doi.org/10.1242/dev.129.12.2851.

Green AC, Martin TJ, Purton LE. 2016. The role of vitamin A and retinoic acid receptor signaling in post-natal maintenance of bone. J Steroid Biochem Mol Biol. 155:135–146. https://doi.org/10.1016/j.jsbmb.2015.09.036.

Harrison EH, Kopec RE. 2020. Enzymology of vertebrate carotenoid oxygenases. Biochim Biophys Acta Mol Cell Biol Lipids. 1865: 158653. https://doi.org/10.1016/j.bbalip.2020.158653.

Helgeland H *et al.* 2014. The evolution and functional divergence of the *beta-carotene oxygenase* gene family in teleost fish—exemplified by Atlantic salmon. Gene. 543:268–274. https://doi.org/10.1016/j.gene.2014.02.042.

Helgeland H *et al.* 2019. Genomic and functional gene studies suggest a key role of *beta-carotene oxygenase 1 like (bco1l)* gene in salmon flesh color. Sci Rep. 9:20061. https://doi.org/10.1038/s41598-019-56438-3.

Hernandez LH, Hardy RW. 2020. Vitamin A functions and requirements in fish. Aquac Res. 51:3061–3071. https://doi.org/10.1111/are.14667.

Hessel S *et al.* 2007. CMO1 deficiency abolishes vitamin A production from β-carotene and alters lipid metabolism in mice. J Biol Chem. 282:33553–33561. https://doi.org/10.1074/jbc.M706763200.

Hu P *et al.* 2008. Retinoid regulation of the zebrafish *cyp26a1* promoter. Dev Dyn. 237:3798–3808. https://doi.org/10.1002/dvdy.21801.

Huang Z *et al.* 2018. Role of vitamin A in the immune system. J Clin Med. 7:258. https://doi.org/10.3390/jcm7090258.

Huang D *et al.* 2021. Development and genetics of red coloration in the zebrafish relative *Danio albolineatus*. eLife. 10:e70253. https://doi.org/10.7554/eLife.70253.

Irie T, Seki T. 2002. Retinoid composition and retinal localization in the eggs of teleost fishes. Comp Biochem Physiol B Biochem Mol Biol. 131:209–219. https://doi.org/10.1016/S1096-4959(01)00496-1.

Isken A *et al.* 2007. Sequestration of retinyl esters is essential for retinoid signaling in the zebrafish embryo. J Biol Chem. 282: 1144–1151. https://doi.org/10.1074/jbc.M609109200.

Isken A *et al.* 2008. RBP4 disrupts vitamin A uptake homeostasis in a STRA6-deficient animal model for Matthew-Wood syndrome. Cell Metab. 7:258–268. https://doi.org/10.1016/j.cmet.2008.01.009.

Kaisuyama M, Matsuno T. 1988. Carotenoid and vitamin A, and metabolism of carotenoids, β-carotene, canthaxanthin, astaxanthin, zeaxanthin, lutein, and tunaxanthin in tilapia *Tilapia nilotica*. Comp Biochem Physiol Part B. 90:131–139. https://doi.org/10.1016/0305-0491(88)90049-1.

Keegan BR *et al.* 2005. Retinoic acid signaling restricts the cardiac progenitor pool. Science. 307:247–249. https://doi.org/10.1126/science.1101573.

Kim Y-K *et al.* 2011. β-Carotene and its cleavage enzyme β-carotene-15,15′-oxygenase (CMOI) affect retinoid metabolism in developing tissues. FASEB J. 25:1641–1652. https://doi.org/10.1096/fj.10-175448.

Kiser PD, Golczak M, Palczewski K. 2014. Chemistry of the retinoid (visual) cycle. Chem Rev. 114:194–232. https://doi.org/10.1021/cr400107q.

Kuehn E *et al.* 2022. Segment number threshold determines juvenile onset of germline cluster expansion in *Platynereis dumerilii*. J Exp Zoolog B Mol Dev Evol. 338:225–240. https://doi.org/10.1002/jez.b.23100.

Downloaded from academic.oup.com/genetics/article/233/1/iyag049/8498880 by Columbia University Libraries user on 04 October 2026

Kuhn BN. 2022. Phenotypic effects of knocking out the pigmentation related genes, *abcg2*, *bco1*, and *bco1-like* in Atlantic salmon [Master's Thesis]. Norwegian University of Life Sciences.

Kwon YM *et al.* 2022. Genomic consequences of domestication of the Siamese fighting fish. Sci Adv. 8:eabm4950. https://doi.org/10.1126/sciadv.abm4950.

Lampert JM *et al.* 2003. Provitamin A conversion to retinal via the β, β-carotene-15,15′-oxygenase (*bcox*) is essential for pattern formation and differentiation during zebrafish embryogenesis. Development. 130:2173–2186. https://doi.org/10.1242/dev.00437.

Le H-GT, Dowling JE, Cameron DJ. 2012. Early retinoic acid deprivation in developing zebrafish results in microphthalmia. Vis Neurosci. 29:219–228. https://doi.org/10.1017/S0952523812000296.

Li H, Tyndale ST, Heath DD, Letcher RJ. 2005. Determination of carotenoids and all-*trans*-retinol in fish eggs by liquid chromatography–electrospray ionization–tandem mass spectrometry. J Chromatogr B. 816:49–56. https://doi.org/10.1016/j.jchromb.2004.11.005.

Liao Y *et al.* 2025. Metabolism, function, molecular mechanism, and application of carotenoids in coloration of aquatic animals. Rev Aquac. 17:e70016. https://doi.org/10.1111/raq.70016.

Lichak MR *et al.* 2022. Care and use of Siamese fighting fish (*Betta splendens*) for research. Comp Med. 72:169–180. https://doi.org/10.30802/AALAS-CM-22-000051.

Lindqvist A, Andersson S. 2002. Biochemical properties of purified recombinant human β-carotene 15,15′-monooxygenase. J Biol Chem. 277:23942–23948. https://doi.org/10.1074/jbc.M202756200.

Lindqvist A, Andersson S. 2004. Cell type-specific expression of β-carotene 15,15′-mono-oxygenase in human tissues. J Histochem Cytochem. 52:491–499. https://doi.org/10.1177/002215540405200407.

Lynch M, Conery JS. 2000. The evolutionary fate and consequences of duplicate genes. Science. 290:1151–1155. https://doi.org/10.1126/science.290.5494.1151.

Magadum S *et al.* 2013. Gene duplication as a major force in evolution. J Genet. 92:155–161. https://doi.org/10.1007/s12041-013-0212-8.

Mashal RD, Koontz J, Sklar J. 1995. Detection of mutations by cleavage of DNA heteroduplexes with bacteriophage resolvases. Nat Genet. 9:177–183. https://doi.org/10.1038/ng0295-177.

Menezes MSS, Almeida CMM. 2024. Structural, functional, nutritional and clinical aspects of vitamin A: a review. PharmaNutrition. 27:100383. https://doi.org/10.1016/j.phanu.2024.100383.

Metibemu DS, Ogungbe IV. 2022. Carotenoids in drug discovery and medicine: pathways and molecular targets implicated in human diseases. Molecules. 27:6005. https://doi.org/10.3390/molecules27186005.

Mora O *et al.* 2004. A potential role for beta-carotene in avian embryonic development. Int J Vitam Nutr Res. 74:116–122. https://doi.org/10.1024/0300-9831.74.2.116.

Moren M, Gundersen TE, Hamre K. 2005. Quantitative and qualitative analysis of retinoids in *Artemia* and copepods by HPLC and diode array detection. Aquaculture. 246:359–365. https://doi.org/10.1016/j.aquaculture.2005.01.017.

Moren M, Næss T, Hamre K. 2002. Conversion of β-carotene, canthaxanthin and astaxanthin to vitamin A in Atlantic halibut (*Hippoglossus hippoglossus L.*) juveniles. Fish Physiol Biochem. 27:71–80. https://doi.org/10.1023/B:FISH.0000021819.46235.12.

Nguyen NTT *et al.* 2022. Genomicus in 2022: comparative tools for thousands of genomes and reconstructed ancestors. Nucleic Acids Res. 50:D1025–D1031. https://doi.org/10.1093/nar/gkab1091.

Noy N. 2010. Between death and survival: retinoic acid in regulation of apoptosis. Annu Rev Nutr. 30:201–217. https://doi.org/10.1146/annurev.nutr.28.061807.155509.

Oberhauser V *et al.* 2008. Ninab combines carotenoid oxygenase and retinoid isomerase activity in a single polypeptide. Proc Natl Acad Sci U S A. 105:19000–19005. https://doi.org/10.1073/pnas.0807805105.

O'Byrne SM, Blaner WS. 2013. Retinol and retinyl esters: biochemistry and physiology. J Lipid Res. 54:1731–1743. https://doi.org/10.1194/jlr.R037648.

Olson JA, Hayaishi O. 1965. The enzymatic cleavage of beta-carotene into vitamin A by soluble enzymes of rat liver and intestine. Proc Natl Acad Sci U S A. 54:1364–1370. https://doi.org/10.1073/pnas.54.5.1364.

Paik J *et al.* 2001. Expression and characterization of a murine enzyme able to cleave β-carotene: the formation of retinoids. J Biol Chem. 276:32160–32168. https://doi.org/10.1074/jbc.M010086200.

Palmiotti A *et al.* 2023. Genetic manipulation of betta fish. Front Genome Ed. 5:1167093. https://doi.org/10.3389/fgeed.2023.1167093.

Petkovich M, Chambon P. 2022. Retinoic acid receptors at 35 years. J Mol Endocrinol. 69:T13–T24. https://doi.org/10.1530/JME-22-0097.

Qian W, Liao B-Y, Chang AY-F, Zhang J. 2010. Maintenance of duplicate genes and their functional redundancy by reduced expression. Trends Genet. 26:425–430. https://doi.org/10.1016/j.tig.2010.07.002.

Rabinowitz JS *et al.* 2017. Transcriptomic, proteomic, and metabolomic landscape of positional memory in the caudal fin of zebrafish. Proc Natl Acad Sci U S A. 114:E717–E726. https://doi.org/10.1073/pnas.1620755114.

Raverdeau M, Mills KHG. 2014. Modulation of T cell and innate immune responses by retinoic acid. J Immunol. 192:2953–2958. https://doi.org/10.4049/jimmunol.1303245.

R Core Team. 2025. R: A language and environment for statistical computing. R Foundation for Statistical Computing, Vienna, Austria. https://www.R-project.org/.

Samarut E, Fraher D, Laudet V, Gibert Y. 2015. ZebRA: an overview of retinoic acid signaling during zebrafish development. Biochim Biophys Acta Gene Regul Mech. 1849:73–83. https://doi.org/10.1016/j.bbagrm.2014.05.030.

Sandell LL *et al.* 2007. RDH10 is essential for synthesis of embryonic retinoic acid and is required for limb, craniofacial, and organ development. Genes Dev. 21:1113–1124. https://doi.org/10.1101/gad.1533407.

Sangeetha RK, Baskaran V. 2010. Retinol-deficient rats can convert a pharmacological dose of astaxanthin to retinol: antioxidant potential of astaxanthin, lutein, and β-carotene. Can J Physiol Pharmacol. 88:977–985. https://doi.org/10.1139/Y10-074.

Sayers EW *et al.* 2024. Database resources of the National Center for Biotechnology Information in 2025. Nucleic Acids Res. 53:D20–D29. https://doi.org/10.1093/nar/gkae979.

Schiedt K, Leuenberger FJ, Vecchi M, Glinz E. 1985. Absorption, retention and metabolic transformations of carotenoids in rainbow trout, salmon and chicken. Pure Appl Chem. 57:685–692. https://doi.org/10.1351/pac198557050685.

Schneider CA, Rasband WS, Eliceiri KW. 2012. NIH image to ImageJ: 25 years of image analysis. Nat Methods. 9:671–675. https://doi.org/10.1038/nmeth.2089.

Sentmanat MF *et al.* 2018. A survey of validation strategies for CRISPR-Cas9 editing. Sci Rep. 8:888. https://doi.org/10.1038/s41598-018-19441-8.

Takitani K, Zhu C-L, Inoue A, Tamai H. 2006. Molecular cloning of the rat β-carotene 15,15′-monooxygenase gene and its regulation by retinoic acid. Eur J Nutr. 45:320–326. https://doi.org/10.1007/s00394-006-0601-3.

Thompson A, Zakon HH, Kirkpatrick M. 2016. Compensatory drift and the evolutionary dynamics of dosage-sensitive duplicate

Downloaded from academic.oup.com/genetics/article/233/1/iyag049/8498880 by Columbia University Libraries user on 04 October 2026

genes. Genetics. 202:765–774. https://doi.org/10.1534/genetics.115.178137.

Tyndale ST, Letcher RJ, Heath JW, Heath DD. 2008. Why are salmon eggs red? Egg carotenoids and early life survival of Chinook salmon (*Oncorhynchus tshawytscha*). Evol Ecol Res. 10:1187–1199.

Vílchez C *et al.* 2011. Marine carotenoids: biological functions and commercial applications. Mar Drugs. 9:319–333. https://doi.org/10.3390/md9030319.

von Lintig J *et al.* 2005. Towards a better understanding of carotenoid metabolism in animals. Biochim Biophys Acta Mol Basis Dis. 1740:122–131. (Carotenoids and Dietary Lipids). https://doi.org/10.1016/j.bbadis.2004.11.010.

von Lintig J. 2010. Colors with functions: elucidating the biochemical and molecular basis of carotenoid metabolism. Annu Rev Nutr. 30:35–56. https://doi.org/10.1146/annurev-nutr-080508-141027.

von Lintig J, Vogt K. 2000. Filling the gap in vitamin A research: molecular identification of an enzyme cleaving β-carotene to retinal. J Biol Chem. 275:11915–11920. https://doi.org/10.1074/jbc.275.16.11915.

Wang X *et al.* 2023. Toxic effects of exogenous retinoic acid on the neurodevelopment of zebrafish (*Danio rerio*) embryos. Neurotoxicol Teratol. 100:107291. https://doi.org/10.1016/j.ntt.2023.107291.

Wang W-D, Hsu H-J, Li Y-F, Wu C-Y. 2017. Retinoic acid protects and rescues the development of zebrafish embryonic retinal photoreceptor cells from exposure to paclobutrazol. Int J Mol Sci. 18:130. https://doi.org/10.3390/ijms18010130.

Ward N, Moreno-Hagelsieb G. 2014. Quickly finding orthologs as reciprocal best hits with BLAT, LAST, and UBLAST: how much do we miss? PLoS One. 9:e101850. https://doi.org/10.1371/journal.pone.0101850.

White JA *et al.* 1996. Identification of the retinoic acid-inducible all-trans-retinoic acid 4-hydroxylase. J Biol Chem. 271:29922–29927. https://doi.org/10.1074/jbc.271.47.29922.

Wilkins LGE *et al.* 2017. Environmental stress linked to consumption of maternally derived carotenoids in brown trout embryos (*Salmo trutta*). Ecol Evol. 7:5082–5093. https://doi.org/10.1002/ece3.3076.

Wilson AE, Liberles DA. 2023. Dosage balance acts as a time-dependent selective barrier to subfunctionalization. BMC Ecol Evol. 23:14. https://doi.org/10.1186/s12862-023-02116-y.

Wyss A *et al.* 2000. Cloning and expression of β, β-carotene 15,15′-dioxygenase. Biochem Biophys Res Commun. 271:334–336. https://doi.org/10.1006/bbrc.2000.2619.

Wyss A *et al.* 2001. Expression pattern and localization of β, β-carotene 15,15′-dioxygenase in different tissues. Biochem J. 354:521–529. https://doi.org/10.1042/0264-6021:3540521.

Yamashita E, Arai S, Matsuno T. 1996. Metabolism of xanthophylls to vitamin A and new apocarotenoids in liver and skin of black bass, *Micropterus salmoides*. Comp Biochem Physiol B Biochem Mol Biol. 113:485–489. https://doi.org/10.1016/0305-0491(95)02069-1.

Yan W *et al.* 2001. Cloning and characterization of a human β, β-carotene-15, 15′-dioxygenase that is highly expressed in the retinal pigment epithelium. Genomics. 72:193–202. https://doi.org/10.1006/geno.2000.6476.

Editor: K. Sampath

Downloaded from academic.oup.com/genetics/article/233/1/iyag049/8498880 by Columbia University Libraries user on 04 October 2026